DISSERTATION

HIV AND ZIKA: MODELING PATHOGENESIS AND THERAPIES IN HUMANIZED MICE

Submitted by

Paige Charlins

Graduate Degree Program in Cell and Molecular Biology

In partial fulfillment of the requirements

For the Degree of Doctor of Philosophy

Colorado State University

Fort Collins, Colorado

Summer 2017

Doctoral Committee:

Advisor: Ramesh Akkina

Howard Liber
Tawfik Aboellail
Elizabeth Ryan

ABSTRACT

HIV AND ZIKA: MODELING PATHOGENESIS AND THERAPIES IN HUMANIZED MICE

Investigation into pathogenesis of critical viral diseases that pose a global threat is important not only for pathogen modeling but also for treatment discovery. Use of humanized mice to study viral pathogens, including HIV-1 and Zika virus, provide a novel insight into the mechanisms of viral persistence and act as a platform for therapeutic intervention and observation. In the context of HIV-1 research, humanized mice are ideal for parroting the infection mechanics. Recapitulation of HIV-1 viral pathogenesis enables the study of various facets of the virus lifecycle, concerning infection establishment, detection, and treatment. In this respect, humanized mouse modeling of HIV-1 infection is paramount for continued studies of HIV-1 in terms of HIV-1 latency, with focus on viral reactivation and outgrowth, and for research with novel therapeutic approaches for treatment and modulation of the infection. The model has been paramount in development of an ultra-sensitive assay for detection of latent HIV-1 and validation of aptamer-siRNA conjugates and conditionally replicating vectors for treatment of HIV-1 infection. Humanized mice can further be expanded for the study of additional emerging pathogens, such as Zika virus, in terms of infection pathology and immune response. Infection of humanized mice with a Puerto Rican strain of Zika virus resulted in high plasma viral loads detectable up to four months post inoculation with wide spread dissemination detected in various tissues by IHC and CLARITY. Understanding these different elements of various viral infections with the ability to establish innovative perspective into mechanics and therapeutics, contribute a previously inaccessible view of human specific viral pathogenesis and treatment.

ACKNOWLEDGMENTS

I would very much like to thank my parents for all your love and unconditional support, without you both I definitely would not be here or of had the courage to pursue and complete this journey. Julia for always being there for me and letting me know that this would be as painful as a kidney stone, but too shall pass. Steven for all your love, support, and for coming home from war and moving half way across the country because after one adventure, who does not like jumping into the next. Howard, your continual guidance has been one of the greatest helps on this journey. Carol, for your support in getting me to the finish line. Tawfik, for all your time working together on multiple projects, it has been quite humbling. Elizabeth, for your support and encouragement through this process. And last but not least the Akkina lab, for all those experiences that you just cannot get out of a textbook.

TABLE OF CONTENTS

INTRODUCTION

The study of human specific viruses is critical as new and reemerging viruses continue to pose a threat to the global community. As emerging pathogens surface and reach epidemic and pandemic status, emphasis is directed towards unearthing a deeper understanding of pathogen modeling in terms of disease mechanisms as well as treatment development and assessment. However, modeling viral pathogenesis in the context of human disease has faced many challenges, including the ability to recapitulate genuine infection mechanisms and investigate innovative therapeutic approaches for infection modulation in a physiologically relevant setting. Many models have been developed for recapitulation of human diseases, from *in vitro* cell lines to *in vivo* animal models. While *in vivo* models, including mice, rats, and nonhuman primates, have permitted investigation into various important viral pathogens, they are limited in their ability to capture complete viral mechanics of human infection. *In vivo* research utilizing mouse models have long been essential for both basic and translational research [1]. Though mice can provide indispensable information regarding disease and treatment, they are limited by their evolutionary differences and their ability to truly recapitulate human specific diseases in a physiologically relevant context. These limitations require broadening the use of nonhuman primate models for infectious disease research. Nonhuman primate models are necessary for collection of preclinical data as the relative nature of the studies can be translated into human clinical studies, providing a solid foundation for expansion of disease and therapeutic research. Unfortunately, the use of these models can be cost prohibitive for large sample sizes and require specialty facilities to manage and handle the primates. In this regard, generation of humanized mice that are capable of mimicking human specific diseases, enables the use of human specific pathogens with much larger sample sizes at a much more reasonable cost than nonhuman primates [2, 3].

Continuous spread of viral infections, such as the continuing HIV-1 pandemic and the reemerging worldwide threat of Zika virus, require exploration into *in vivo* models that are capable of mimicking

human disease progression and therapeutic interventions [4, 5]. To address this need, humanized mice have been established as an indispensable model for the study of human specific viral pathogenesis. Humanized mice harbor a complete human immune system, generated by transplantation of human peripheral blood mononuclear cells (PBMC), hematopoietic stem cells (HSC), or the combination of a human tissue xenograft in addition to hematopoietic stem cells (Fig 1) [6]. These human immune cells, including both myeloid and lymphoid lineages, home to their relevant physiological location within the mouse. This homing allows repopulation of lymphoid tissues such as the spleen, lymph nodes, gut and reproductive tract mucosa, in addition to systemic leukocyte reconstitution [7]. These mice allow for human pathogenesis to be observed due to the natural spread of the viral infection through its primary tissue reservoirs eliciting both an innate and adaptive immune response in the humanized mouse. This method of human cell transplantation permits the research of human specific pathogens, from HIV to Zika, for the study of infection progression, immune response, and treatment strategies [8, 9].

Humanized Mouse Models

Initial generations of humanized mice relied on the use of severe combined immunodeficient (SCID) mouse background [10]. These mice maintained an innate immune system but lacked T cells and B cells, which permit the transplantation of human immune cells with reduced tissue rejection [11, 12]. The humanized SCID mouse then evolved by inclusion of both transplantation of human fetal thymus under the mouse kidney capsule and subsequent injection of autologous hematopoietic stem cells directly into the xenograft [13]. Though complete immune cell reconstitution was limited, this model enables the study of HIV-1, with the predominant immune cell phenotype consisting of CD4 T cells. The SCID genetic background was crossed with the non-obese diabetic (NOD) background, resulting in an increase in engraftment levels of human cells [14]. Later generations of immunocompromised mice included those that completely lacked all mouse B cells, T cells, and NK cells [15]. These mice were engineered to contain knockouts of the Rag1 or Rag2 gene, with later models containing knockouts for IL-2 receptor common

gamma chain gene [16-18]. A predominate genotype currently used for generation of humanized mice consists of BALB/c-Rag1^{null}Iγc^{null} or BALB/c-Rag2^{null}γc^{null}, which combines the best current genetic background promoting increased levels of human immune cell engraftment and differentiation [19]. These genetic knockout mice resulted in increased levels of human cell engraftment as well as the ability to represent a more complete innate and adaptive immune response, as immune cell reconstitution now included human NK cells, dendritic cells, monocytes, macrophages, granulocytes, T cells, and B cells. The BALB/c-Rag1^{null}γc^{null} or BALB/c-Rag2^{null}γc^{null} genetic backgrounds have been successfully used for generation of multiple humanized mice models, chiefly the huPBL, huHSC, and BLT models (Fig 1) [3, 20].

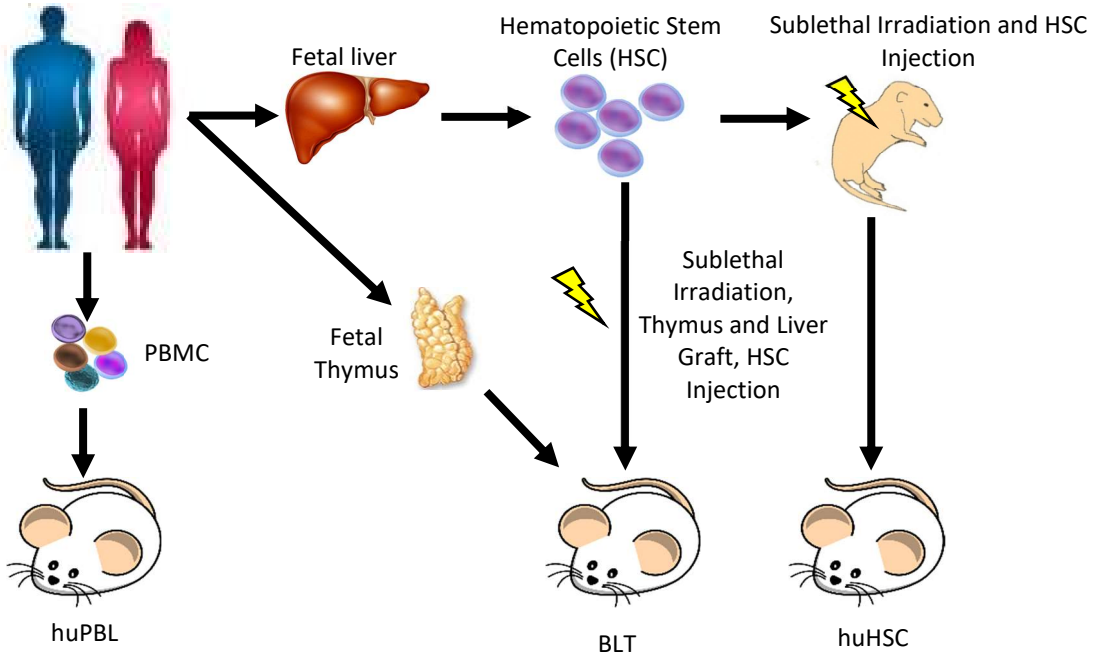

Figure 1 Generation of Humanized Mouse Models

huPBL Mouse Model

The huPBL model, humanized by peripheral blood mononuclear cells (PBMC), utilize adult immunodeficient mice with the genetic background BALB/c-Rag1^{null}γc^{null} or BALB/c-Rag2^{null}γc^{null}, that are then injected intraperitoneally with human PBMC. Though incapable of multilineage hematopoiesis, as this mouse is transplanted with a finite number of mature human immune cells, this model contains human T cells, B cells, monocytes, macrophages, dendritic and natural killer cells. As these mice do not

require preconditioning by sublethal radiation prior to engraftment of PBMC, these mice are straightforward to generate and can produce cohorts of humanized mice from a multitude of donors, which promotes a wide variety of donor variation during experimentation. This model is ideal for studying gene therapy strategies as transplanted cells can be modified prior to infusion into the mice [21, 22]. While the ease of huPBL generation and ability to use multiple donors to generate the transplanted human immune system is advantageous, this model is limited by the wide donor cell variation affecting engraftment levels and the development of graft versus host disease with long term use of this model [23].

huHSC Mouse Model

Another model that utilizes the transplantation of a complete immune system into immunodificient mice are the humanized by hematopoietic stem cell (huHSC) mice [24]. Using the same immunodeficient genetic background stated above, these mice are sublethally irradiated as neonates, typically 1-4 day old pups, then injected intrahepatically with human hematopoietic stem cells (HSC). These cells undergo multilineage hematopoiesis and repopulate the mouse with a complete human immune system, including both myeloid and lymphoid lineages (Fig 2) [25]. In contrast to the huPBL model, the HSC's in these humanized mice sustain de novo hematopoiesis and, due to the preconditioning

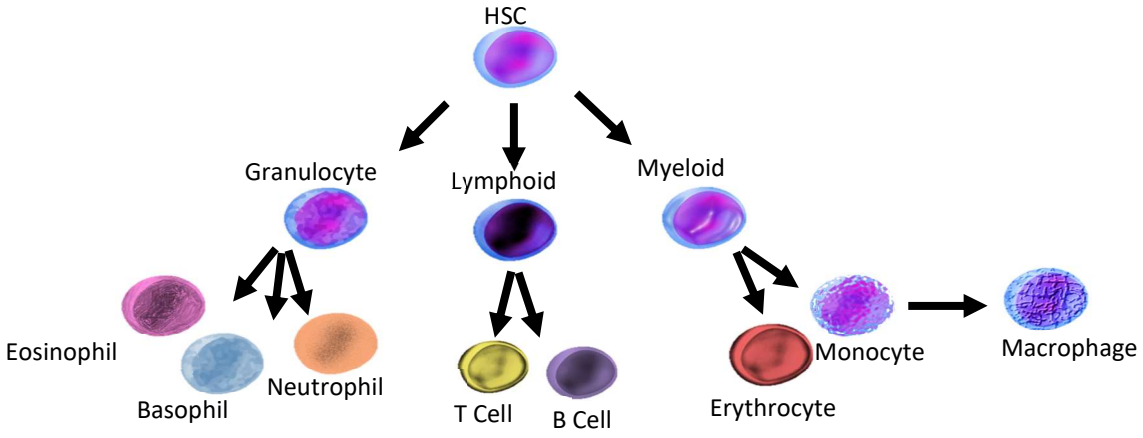

Figure 2 Humanized Mouse Immune Cell Reconstitution. Hematopoietic stem cell differentiation pathways present *in vivo.*

irradiation and engraftment with stem cells, graft versus host disease is minimal to nonexistent. Engraftment of the mice, determined by expression of leukocyte common antigen (CD45) of the total mouse leukocyte population, is comprised of human T cells, including both cytotoxic T cells and helper T cells, B cells, monocytes, macrophages, granulocytes, dendritic cells, and NK cells [7, 26].

Infection of huHSC mice with human specific pathogens by various routes, including intraperitoneal, intravenous, subcutaneous, and mucosal transmission, is permitted due to repopulation of human cells in the tissues of the transplanted mice [26]. Multiple studies have shown the presence of human leukocytes in the spleen, lymph nodes, and reproductive tract in huHSC mice [27-29]. As engraftment can persist more than six months to a year in this model, infectious disease experiments can be sustained in these mice for multiple months [30]. This is highly advantageous for long-term chronic infection studies where disease progression, as demonstrated by HIV-1 CD4 T cell decline or antibody production to combat Zika infection, can be observed.

BLT Mouse Model

Expanding on the huHSC model, is the bone marrow-liver-thymus (BLT) model. The most notable improvement in this model when compared to the previous two, is the addition of a human fetal liver and thymus tissue graft placed under the kidney capsule of the immunodeficient adult mice [31]. These mice are then injected intravenously with autologous HSC derived from fetal liver tissue. Very similar to the huHSC model, BLT mice sustain de novo multilineage hematopoiesis, with the primary advantage being an enhanced T cell population with the ability for T cell education and restriction due to the presence of a human thymus graft. Application of these humanized mouse models to the study of HIV-1 and Zika have dramatically changed the field [32]. More relevant translational studies can be conducted, expanding on the information gathered *in vitro* thus reducing the reliance on costly non-human primate models [33, 34]. In a groundbreaking study, as discussed in a later chapter, BLT mice have provided novel insight into

the pathogenesis of the Zika virus as the level of engraftment and more complete immune responses to infection provide a solid foundation for the investigation of emerging viral threats [35].

Human Pathogen Research Involving Humanized Mice

Pathogen research, with emphasis on human-specific viruses, has been greatly advanced using humanized mice. The most notable viruses that have greatly benefited from the development of these models include HIV-1, HTLV-1, dengue, Epstein-Barr virus, Hepatitis C virus, and the reemerging Zika virus [4, 8, 36-38]. Use of humanized mice have been instrumental in infectious disease research as many human pathogens are not able to infect mice, nonhuman primates, or other laboratory animal species, thus requiring either viral modification or interpretation for translational application. The huPBL, huHSC, and BLT models successfully permit viral infection by intraperitoneal and intravenous challenges, with the latter of the two models successfully demonstrating infection by subcutaneous and mucosal challenges as well [4, 24, 39]. Cellular and humoral immune responses are seen in both the huHSC and BLT models, antigen specific IgM production observed in the huHSC and BLT models, with the advantage of the BLT model producing a more complete humoral response [40, 41]. Novel experimental approaches can be conducted permitting an extensive understanding of disease pathogenesis, immune response, and therapeutic approaches.

HIV-1 Research in Humanized Mice

Foundational studies involving HIV-1 infection of humanized mice demonstrated susceptibility, chronic infection, and characteristic CD4 T cell decline with both the CCR5 and CXCR4 tropic strains of HIV-1 [7]. These studies revealed that humanized mice were susceptible to infection by both intraperitoneal and mucosal inoculation. Acute and chronic infection closely mimicked that of HIV-1 human disease with the quintessential peak in HIV-1 viral RNA plasma loads during acute infection and CD4 T cell decline noted over the course of the study. As these mice harbor complete immune system susceptible to HIV-1 infection, a recent study that will be discussed in a later chapter, has demonstrated the ability for viral

outgrowth in humanized mice that are infused with HIV-1 positive donor cells for detection of latent virus. With a focus on humoral response, a different study observed production of both HIV-1 envelope gp-120 and p24 capsid specific antibodies in huHSC mice generated from fetal cord blood derived CD34 HSC [42]. BLT mice used in the study of HIV-1 infection have also demonstrated antibody production during infection, suggesting that these models may play a pivotal role in HIV-1 vaccine development [40]. In addition to cellular and humoral responses seen during HIV-1 infection, humanized mice mimicry of HIV-1 dissemination permits investigation into HIV-1 viral tissue reservoirs [34].

In recent years, the humanized mouse model of HIV-1 infection has been expanded to explore antiretroviral therapeutics. Studies of antiretroviral drugs, novel antiretroviral agents, and gene therapy approaches have been investigated in the humanized mouse model and have provided necessary information that has been vital for translational medical research. These experiments included optimization of antiretroviral therapeutics, such as raltegravir, tenofovir, miraviroc, or broadly neutralizing antibodies, as either a preexposure prophylaxis or post infection treatment [24, 27, 28, 43]. Novel antiretroviral approaches have included the use of RNA-based aptamer and aptamer-siRNA conjugates for modulation of infection and cell to cell transmission [44-49]. One such study, utilizing CXCR4 tropic HIV-1, successfully demonstrated the effectiveness of an RNA-based aptamer, as well as that of an RNA-based aptamer-siRNA conjugate, in decreasing HIV-1 viral loads and preserving CD4 T cell levels during the duration of treatment in humanized mice[48]. A recent study expanding on the use of aptamer-siRNA conjugates for modulation of HIV-1 infection through virus neutralization and transcriptional and post-transcriptional regulation, will be discussed in a later chapter.

Beyond the use of systemically administered therapeutics, investigation into the use of gene therapy as a means for treatment and potential cure for HIV-1 has been expanded. Multiple approaches using modified immune cells for the generation of huPBL mice for HIV-1 modulation have shown success. Focus on the HIV-1 co-receptor's, CCR5 or CXCR4, *in vivo* studies using huPBL mice showed significant

potential as a means for augmentation of donor derived CD4 T cells for resistance to HIV-1 infection [21]. Studies have demonstrated zinc finger nucleases as a viable method for HIV-1 CCR5 co-receptor knockdown in CD4 T cells. Disruption of CCR5 by ZFN is an attractive therapeutic as the chemokine receptor is required by myeloid-tropic HIV-1 for infection, with the vast majority of transmission events occurring from this viral type [22]. People with demonstrated homozygous CCR5 delta 32 mutations, which inhibit receptor translocation to the plasma membrane, render the individuals resistant to HIV-1 CCR5 specific HIV infection. The success of CCR5 disruption recently translated to a first-of-its-kind clinical trial using zinc finger modification to disrupt CCR5 in autologous patient CD4 T cells, which were later infused back into the patient [50, 51]. This resulting modification increases the patients' resistance to infection and, when removed from ART, viral rebound was slowed in comparison to unmodified cells.

Successful use of huPBL mice to study HIV-1 treatment development has also led to the investigation of lentiviral vectors for the treatment of HIV-1 infection. Current studies using lentiviral vectors as means for delivery of siRNA payloads for small interfering RNA-dependent modulation of both viral and innate cell gene transcripts have shown success and will be discussed later [52-54]. Expanding on the use of single round lentiviral vectors has been the development of conditionally replicating vectors. These conditionally replicating vectors are constructed using a lentivirus backbone with modifications resulting in its ability for transcription and repackaging being dependent upon HIV-1 infection. These vectors aim to functionally modulate HIV-1 infection without the requirement of any other external treatments. A previous study, observing the ability of this tool to conditionally replicate, showed promising results [55, 56]. Recently, novel conditionally replicating vectors have been engineered to include siRNA or CRISPR/Cas payloads for disruption of intracellular HIV-1 infection. To be discussed in detail in a later chapter, huPBL mice were generated by the transplantation of lentiviral vector modified human CD4 T cells harboring these anti-HIV constructs. Cell donor variation and strength of these anti-HIV constructs introduced into the modified

cells to inhibit infection varied between treatment groups and translational ability of this approach to clinical studies will be discussed.

Flavivirus Research Utilizing Humanized Mice

Continual expansion of humanized mice for viral pathogenesis studies have broadened to include other families of virus, such as flaviviruses. Dengue, a notable and highly impactful flavivirus, has been extensively studied in humanized mice [57, 58]. One study demonstrated the ability for viral infection as well as a humoral antibody response against the dengue virus in huHSC mice [8]. With viremia lasting for up to 3 weeks and anti-dengue IgG and IgM production detected in mouse serum, the results provide exciting new insight into the use of humanized mice for dengue immunopathogenic studies. This study paved the way for another flavivirus, Zika virus, to be studied. Zika virus is currently posing a global threat due to its unknown mechanisms of transmission, infection kinetics, and lack of effective treatment therapies. Investigation into Zika virus pathogenesis has skyrocketed in recent years, fielding efforts to establish an *in vivo* model for recapitulation of viral infection and transmission [35]. Current models using immunocompromised mice and nonhuman primates have been instrumental in elucidating infection kinetics, cell and tissue targets, and maternal-fetal transmission [59]. However, the genetic engineering of the various mouse models inadequately models natural infection mechanics, while nonhuman primates, though capable of cellular and humoral responses, are quite costly and are limited by sample size. In this regard, the use of humanized mice that contain an innate and adaptive immunity capable of eliciting both a cellular and humoral response, are providing critical insight into Zika pathogenesis. Ongoing research utilizing huHSC and BLT mice, that will be discussed in a later chapter, has revealed that humanized mice are susceptible to Zika virus infection, can sustain viral infection for greater than 4 months, can produce Zika specific antibodies, and can provide unprecedented insight into virus tropism and dissemination through histological analysis.

By direct injection of human peripheral blood mononuclear cells or hematopoietic stem cells into genetically modified immunodeficient mice, high levels of complete human immune system reconstitution have enabled the studies of human specific virus infection, such as HIV-1, as well as increased the field's understanding of global viral threats such as the reemerging Zika virus. Application of humanized mice for the study infectious diseases facilitate translational research as a powerful tool for investigation into biological mechanisms and preclinical testing.

PART I

MODELING HIV PATHOGENESIS AND THERAPIES IN HUMANIZED MICE

CHAPTER 1

ULTRASENSITIVE HUMANIZED MOUSE VIRAL OUTGROWTH ASSAY FOR QUALIFICATION OF LATENT HIV-1 RESERVOIRS

As progressive therapies for the treatment and cure of HIV-1 continue to intensify, a crucial need for ultrasensitive assays to detect latently infected cells has arisen. HIV-1 latently infected cells, which consist of dormant, replication competent cells, remain the predominant hurdle in complete virus eradication. Thus, a highly sensitive assay for detection of this population is critical. Current detection methods for determination of the latently infected cell population size include PCR for integrated virus and the gold standard quantitative viral outgrowth assay (qVOA). Inherent to these methods are their nature to overestimate or underestimate the size of the latent reservoir. Furthermore, these tests were unable to detect virus in patients such as the "Boston Patients" and "Mississippi Baby". Our aim is to investigate alternative approaches for sensitive viral detection. In this regard, the humanized mice provide an optimal *in vivo* setting to obtain viral outgrowth due to their permissiveness for viral infection, as well as latency and viral reactivation. We aim to establish a viral outgrowth in humanized mice from peripheral blood CD4 T cell samples from HIV-1 positive patient samples with low to no detectable viral loads by qRT-PCR in patient plasma samples or by the standard qVOA. In the initial standardization of the hmVOA assay, patient samples wherein virus was detected by the *in vitro* qVOA, were all positive for viral outgrowth in the humanized mice. In subsequent validation of hmVOA sensitivity, four out of the five patient samples that were negative by the qVOA were positive for viral outgrowth *in vivo*. Our results advocate the use of humanized mice as a sensitive means for determination of viral outgrowth from samples that are negative by other means.

Introduction

The advancement of effective antiretroviral therapy (ART) has greatly helped in diminishing both viral transmission and disease progression [60]. However, ART is unable to achieve a complete cure as

latent cells, cells that have nonproductive infection, remain elusive from both immune and drug therapies [61]. HIV-1 requires a specific tropism for infectivity of human cells, necessitating expression of the receptor CD4 as well as a chemokine receptor, either CXCR4 or CCR5, for viral entry into the cell. Cell types known to express CD4 and either co-receptor include CD4 T cells, macrophages, glial cells, dendritic cells, and to a rare extent CD34 hematopoietic stem cells [62]. CD4 T cells are the most prominent cell reservoir that have been identified as harboring latent HIV provirus and present a formidable barrier for viral eradication [63, 64]. These cell types, which are dispersed throughout a variety of tissues in the human body, have been demonstrated to harbor integrated HIV-1 DNA and represent latent cell reservoirs [65-67]. Though quite a few cell phenotypes can become infected with HIV-1, the prevalence of latently infected cells can be as small as one infected cell out of 1 million CD4 memory T cells, increasing the difficulty in identifying this reservoir. Thus, current strategies are aimed at reactivation of latent cells by novel drug approaches with the objective of eliminating these cells by triggering recognition from the immune system [68, 69]. Though advancements have been made in the discovery of novel drug and antibody therapeutics, the ability to ascertain the presence, size, and location of latent cell reservoirs in HIV-1 positive individuals remain difficult as multiple cell and tissues reservoirs exist for the latent cells.

Current detection methods for identification of latently infected cells that utilize PCR identification of integrated DNA globally overestimate the size of the latent reservoir as not all integrated provirus is replication competent [70]. This can be due to epigenetic modifications or integration site of the provirus. Standard PCR assays are only capable of looking at integrated HIV proviral DNA, while qRT-PCR and now ddPCR with an increased sensitivity, can quantify systemically present viral RNA with a sensitive but limited limit of detection. Additionally, qRT-PCR relies on viral activation and production for detection of HIV-1 infection in individuals. Challenges with this assay are encountered when patients who have been on long-term ART therapy have viral loads below the limit of detection, though the presence of latently infected cells still exists during this time. In this regard, a sensitive assay that is able to distinguish between

replication competent and incompetent virus and detect the presence of an incredibly small latent HIV reservoir is crucial, as only the replication competent latent virus is responsible for viral rebound necessitating treatment. Currently, determination of the replication competent latent reservoir size relies on the gold standard quantitative viral outgrowth assay (qVOA) [69, 71]. The frequency of latently infected CD4 T cells is measured by stimulation of CD4 T cells from HIV-1 positive donor samples that are then cocultured *in vitro* with allogenic CD8 depleted HIV-1 negative donor peripheral blood mononuclear cells (PBMC). This assay relies on the production and expansion of mature HIV-1 virions in the culture that are then detected by qRT-PCR of viral RNA or by p24 ELISA of the viral capsid protein. The assay is able to statistically derive the infectious units per million (IUPM) cells to estimate the size of the latent cell population [70].

As the field of HIV shifts towards developing curative strategies, the ability to determine the size of the latent reservoir in patients on highly active antiretroviral therapy and more recently the success of those patients that have undergone allogenic stem cell transplant, are currently limited to PCR and the *in vitro* qVOA. The most notable case of HIV-1 curative therapy is that of the Berlin patient. An HIV-1 positive male, who in addition to HIV-1 infection also had adult T-cell leukemia, underwent an allogenic stem cell transplant utilizing stem cells that were homozygous for the CCR5 delta 32 mutation rendering cells incapable of HIV-1 infection by CCR5 tropic virus. After receiving the transplant, all subsequent qRT-PCR and qVOA assays of the patients' plasma and cell samples were negative. This then led to analytical treatment interruption (ATI) to observe if the patient was fully cured. After more than eight years, the Berlin patient has been negative for HIV-1 by any current assay. However, the significance of the qVOA limitations were observed when the assay failed to detect replication competent latent HIV-1 in the more recent "Boston patients" and "Mississippi baby". With the objective of recapitulating the Berlin patients' success, two HIV-1 positive patients who underwent an allogenic stem cell transplant, the "Boston patients", had undetectable virus by the gold standard qVOA post-transplant, which led to ATI.

Unfortunately, virus eventually rebounded in these individuals [72]. The “Mississippi baby”, born to an HIV-1 positive mother, began ART within 30 hours of birth in hopes of prohibiting the establishment of the viral reservoir. No virus could be detected during the period of ART therapy as well as for the proceeding 27 months following ATI [73]. Just as in the case of the Berlin patients, virus rebounded in the Mississippi baby [74].

Though the qVOA is the current gold standard, the “Boston patients” and “Mississippi baby” examples reveal the limitations in the ability of the qVOA to identify and estimate the size of the latent reservoir. The first of which encompasses the notion that other tissue reservoirs, in addition to the circulating peripheral blood derived CD4 T cell population, are known to harbor latently infected cells; these well-documented tissue sites include lymph nodes, gastrointestinal and reproductive tract mucosa, and brain. Furthermore, incomplete viral reactivation due to the stimulation method used and duration of the qVOA assay greatly limit the assay. Thus, the need for more sensitive assay for detection of latently infected replication competent cells has arisen.

To address this need, we developed a humanized mouse viral outgrowth assay for detection of latent virus from HIV-1 positive donors that are negative by the standard qVOA. Humanized mice, that contain a complete transplanted human immune system, are ideal models for development of an ultrasensitive viral outgrowth assay. To generate humanized mice, neonatal BALB/c-Rag1$^{null}\gamma c^{null}$ or BALB/c-Rag2$^{null}\gamma c^{null}$ mice were transplanted with human CD34 positive hematopoietic stem cells, resulting in de novo generation of human lymphoid and myeloid immune cells [3]. These mice have the advantage of harboring primary cellular targets of HIV-1 that can sustain HIV-1 infection for greater than one year. BLT mice were also used in addition to the huHSC mice as they have higher T cell reconstitution. However, no difference in the sensitivity for viral outgrowth was observed between the two models. Utilization of the humanized mouse model allows for HIV-1 positive donor CD4 T cells to be cultured in a

physiologically relevant environment that promotes viral reactivation and infection expansion over a longer period of time than the traditional qVOA allows.

HIV-1 positive donor CD4 T cells were used for direct comparison of the qVOA to the hmVOA (Fig 3). CD4 T cells for the initial optimization and validation of the humanized mouse viral outgrowth assay (hmVOA) consisted of CD4 T cells isolated from HIV-1 positive donor PBMC samples that had positive outgrowth by the qVOA. These donors have been on ART and have low to undetectable virus for at least 1 year as determined by qRT-PCR of patient plasma. Further determination of the hmVOA sensitivity utilized donor CD4 T cell samples that were negative by the qVOA. Humanized mice were infused with HIV-1 positive donor CD4 T cells and monitored weekly for viremia by qRT-PCR. Our results from the study validate the use of humanized mice as a more sensitive viral outgrowth assay for determination of latently infected replication competent cells.

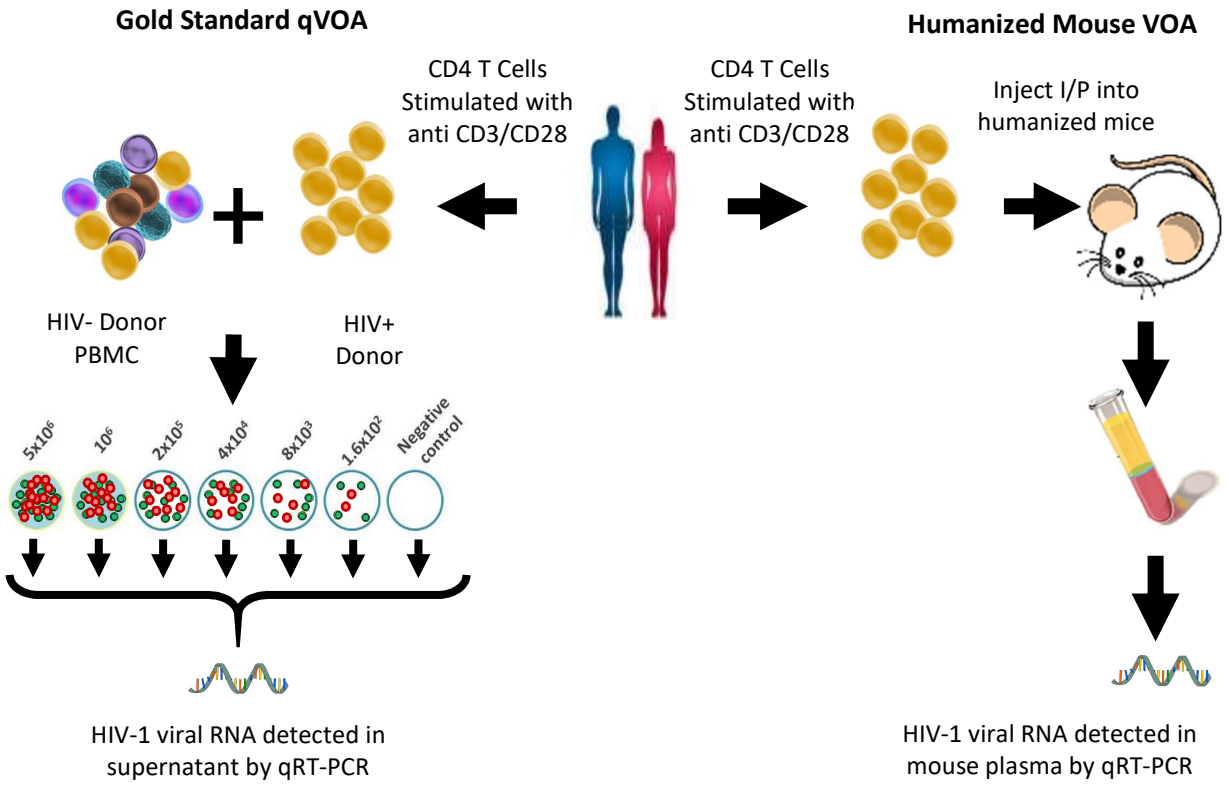

Figure 3 Schematic of Experimental Design for Comparison of qVOA to hmVOA. CD4 T cells are isolated from HIV-1 positive individuals and used for direct comparison of viral outgrowth capacity by qVOA and hmVOA.

Methods

Patient samples and resting CD4+ T cell isolation: To develop and evaluate the hmVOA, we obtained CD4+ T cells from two groups of patients from the Zuckerberg San Francisco General Hospital and the Brigham and Women's Hospital. One group included HIV-1-infected individuals on ART but with intermittent or persistent low-level viremia (<1000 HIV-1 RNA copies/ml of plasma) and the other included individuals on fully suppressive ART with no detectable VL >50 copies/ml at the time of sampling. Institutional approval was obtained from both UCSF and The Brigham and Women's Hospital for collecting samples and conducting this study. Written informed consent was obtained from all study participants. PBMCs were collected from peripheral blood and purified by Ficoll-Hypaque (Sigma-Aldrich) density gradient centrifugation followed by cryopreservation for later testing. Untouched, total CD4+ T cells were purified by negative selection as described previously (95% pure) using antibody coated magnetic beads (Stem Cell Technologies, Vancouver, Canada).

Quantitative viral outgrowth assay: A modified version of an *in vitro* qVOA was performed based on a previously described method using duplicate wells for serial dilutions of 5 million to 0.1 million for each patient sample [75, 76]. Exact dilutions used were based on the number of viable CD4+ T cells that were able to be obtained. Cells were stimulated using αCD3/αCD28 antibodies for up to 21 days in the presence of CD8+ T-cell-depleted blasts obtained from HIV-uninfected blood donors. Positive wells were determined by increasing HIV-1 unspliced (us) RNA detected in assay supernatants over time. HIV-1 RNA was quantified using a Taqman real-time polymerase chain reaction (PCR) method based on previously described primer and probe sequences that amplify of a conserved region in the LTR/gag that is specific to nearly all group M HIV-1 sequences [77]. Briefly, 10 µL of RNA were added to 10 µL of TaqMan® Fast Virus 1-Step Master Mix (ThermoFisher) incorporating forward primer, 5'-TACTGACGCTCTCGCACC, reverse primer, 5'-TCTCGACGCAGGACTCG, and probe, 5'-FAM-CTCTCTCCTTCTAGCCTC-MGB, as per manufacturers protocol followed by thermocycling with an annealing temperature of 60ºC using the

LightCycler 96 system (Roche). The IUPM were calculated for each of the samples positive for viral outgrowth using a maximum likelyhood method and online calculator as described [70]. Cells from the same collection time points were later subjected to hmVOA as described below.

Generation of humanized mice: Immunodeficient Rag1 or Rag2-deficient mice were used to generate humanized mice as previously described [7]. Briefly, huHSC mice were generated by using BALB/c-Rag1^{null}γc^{null} or BALB/c-Rag2^{null}γc^{null} background mice. 1-4 day old neonates were irradiated at a non-lethal dose of 350 rads up to 24 hours prior to engraftment. Human fetal liver-derived CD34 positive hematopoietic stem cells (HSC) cells were purified and cultured for 24 hours in cytokine media [24]. Pups were injected intraheptatically with 0.3-1.0x10^6 human CD34 positive hematopoietic stem cells. 8-12 weeks after injection, mice were screened for engraftment. Peripheral blood was collected and the red blood cells were lysed using the Whole Blood Erythrocyte Lysing Kit (R&D Systems, Minneapolis, MN). Engraftment was determined by the presence of human CD45, human CD3, and human CD4 cells by flow cytometry using the BD Accuri C6.

BLT humanized mice were prepared by transplantation of fragments of human fetal liver and thymic tissues under the mouse kidney capsule followed by tail vein injection of autologous fetal CD34 HSCs as described previously [24]. Transplanted mice were screened for human cell engraftment at 10-12 week post-reconstitution. Peripheral blood was collected and the red blood cells were lysed using the Whole Blood Erythrocyte Lysing Kit (R&D Systems, Minneapolis, MN). Human cell engraftment was determined by the presence of human CD45, human CD3, and human CD4 cells by flow cytometry using BD Accuri C6 [78]. All mice were maintained at the CSU Painter Animal Center. These studies have been reviewed and approved by the Institutional Animal Care and Use Committee.

Humanized mouse viral outgrowth assay model: Cryopreserved purified CD4 positive T cells from known HIV-1 positive donors, which were also used in the qVOA, were used for determining viral outgrowth in humanized mice. Cells were thawed and allowed to recover for a minimum of 4 to 6 hours

in RPMI containing 10% heat inactivated FBS, 2mM L-glutamine, and 5ng/mL IL-2 at 37°C with 5% CO2. Cells were either left unstimulated, or stimulated by the addition of phytohemagglutinin at 2µg/mL or the addition of CD3 and CD28 soluble antibody at 100ng/mL. Cell count and viability was determined prior to injection. Cells were aliquoted at desired live cell number for each humanized mouse to be injected. Mice were infused with the donor cells by intraperitoneal injection with total live cell numbers ranging from 0.1 to $20x10^6$ cells. Mice were monitored for eight weeks, with weekly plasma collections for determination of viral loads by qRT-PCR.

HIV-1 viral loads in humanized mice: HIV-1 viral loads were determined by qRT-PCR analysis of mouse plasma RNA following a protocol previously described [79]. RNA was extracted from 30 µL of mouse plasma following the Omega E.Z.N.A. viral RNA extraction kit per the manufacturer's instructions. HIV-1 viral loads were quantified by using the iTaq Universal Probes kit. Briefly, 8µl of RNA were tested for the presence of HIV-1 using primer and probe sequences targeting the HIV-1 LTR: HIV-1 LTR Forward Primer -5'GCCTCAATAAAGCTTGCCTTG3' at 500nM, HIV-1 LTR Reverse Primer-5'GGCGCCACTGCTAGAGATTTT3' at 500nM, and HIV-1 LTR Probe-5'FAM/AAGTAGTGTGTGCCCGTCTGT3' at 200nM. Samples were ran using a Bio-Rad C1000 Thermal Cycler with a CFX96 Real-Time System. Viral loads were quantified by comparison with an HIV-1 LTR standard curve.

Results

Humanized mice permit latent HIV-1 viral outgrowth from qVOA positive samples: Initial validation experiments were conducted using CD4 T cells from HIV-1 positive donors that had detectable viral outgrowth from the *in vitro* qVOA. Donors were on ART for a minimum of one year and had low but detectable viral loads as well as a known IUPM as determined by qVOA. Cryopreserved CD4 T cell number availability varied between donors and thus cell number injected per mouse was determined accordingly. Humanized mice were injected with donor CD4 T cells and followed for a minimum of eight weeks to determine if there was successful viral outgrowth. Out of the five qVOA positive donors that were used to

validate optimal cell number range infused and stimulation method, all five demonstrated positive viral outgrowth in the humanized mouse viral outgrowth assay model (Table 1).

Table 1 Standardization of hmVOA with qVOA Positive Samples

Donor	Total Cells (Millions)	Range of Cell Number Injected per Mouse (Millions)	Number of Mice Used	Number of Mice with Viral Outgrowth
2	26	0.5-10	9	2
5	34	0.5-20	8	1
8	24	0.1-10	11	5
9	54	0.1-20	13	6
13	24	0.1-10	11	3
15	24	0.1-10	11	4

The initial set of donors were used to optimize the minimum number of cells required for viral outgrowth as well as the optimal stimulation method for viral reactivation. As expected, the larger number of cells injected into the humanized mouse typically resulted in detectable viral outgrowth often at an early week post infusion than smaller cell numbers. Donor 2 had cell numbers injected ranging from 0.5 to 10 million cells per mouse. Cells were left either unstimulated, wherein positive viral outgrowth was observed in one out of 2 mice injected with 5 million unstimulated cells, or stimulated with PHA, that resulted in positive viral outgrowth from 1.25 million stimulated cells. qVOA data from this donor showed that one out of 2 wells containing 5 million HIV-1 positive donor cells became positive, resulting in an IUPM of 0.102. Donor 5 CD4 T cells were also used unstimulated and PHA stimulated, with injected cell numbers ranging from 0.5 to 20 million cells per mouse. One out of 2 mice injected with 1 million

unstimulated cells had positive viral outgrowth in humanized mouse, similar to the qVOA that had positive outgrowth from one out of 2 wells containing 1 million donor cells, resulting in an IUPM of 1.083. Initial data suggest that the hmVOA is as sensitive as the qVOA and that prior stimulation of the donor cells decreases the minimum number of cells needed to observe viral outgrowth in humanized mice. This stimulation increases the opportunity to capture replication competent virus by the hmVOA and better quantify the number of replication competent infectious units that are present in the CD4 T cell reservoir by qVOA.

Based upon the prior stimulation data, all subsequent donor cells were stimulated prior to infusion into the humanized mice. To increase cell viability and overall level of CD4 T cell activation, antihuman CD3 and antihuman CD28 soluble antibodies were used to elicit viral reactivation. For Donor 8, Donor 9, Donor 13, and Donor 15, cells were injected between 0.1 and 20 million cells per mouse depending upon available number of CD4 T cells. Positive viral outgrowth was observed from all for donors, with the highest cell number injected per mouse having positive viral outgrowth for each donor as expected. In addition, Donor 8 had successful viral outgrowth from 0.5, 1, and 5 million cells in addition to the highest number of injected cells, 10 million. Donor 9, in addition to the highest cell number injected mouse of 20 million, had mice injected with 0.5, 1, 5, and 10 million cells become positive for viremia. Similarly, Donor 13 had viral outgrowth from mice injected with 5 and 10 million cells, and Donor 15 had detectable viral outgrowth from mice injected with 0.1, 0.5, 5, and 10 million cells. Donor 8, Donor 9, and Donor 13 had positive viral outgrowth from the qVOA, with IUPM data of 4.468, 1.171, and 3.74, respectively. Donor 15 had no *in vitro* data. HIV-1 viral outgrowth was successfully detected using the humanized mouse viral outgrowth assay from all qVOA positive donor samples.

Positive viral outgrowth observed in humanized mice from patients that are negative by qRT-PCR and qVOA: Following optimization of the humanized mouse viral outgrowth assay with donor samples that were positive by qVOA, HIV-1 positive donor samples that were negative by all current

assays, primarily qRT-PCR of patient plasma and qVOA of isolated CD4 T cell samples, were used to determine if the hmVOA could detect viral outgrowth. HIV-1 positive donor CD4 T cell samples first underwent the *in vitro* qVOA. Those donors that had no detectable viral outgrowth in any well were infused into mice as previously described using the antihuman CD3 and antihuman CD28 stimulation method. Cell numbers injected per mouse depended upon the available number of total CD4 T cells per donor.

Table 2 hmVOA using qVOA Negative Samples

A total of 5 donors were used to ascertain if the hmVOA is more sensitive than the gold standard qVOA. Successful viral outgrowth was observed in 4 out of the 5 donors used (Table 2).

Donor	Total Cells (Millions)	Range of Cell Number Injected per Mouse (Millions)	Number of Mice Used	Number of Mice with Viral Outgrowth
30	32	2-10	6	1
32	16	4	4	1
34	17	4.25	4	1
41	15	5	3	0
42	27	5-7	5	3

As all these donors were negative by the *in vitro* qVOA, the maximum number of cells injected per mouse in the largest number of replicates was optimized per donor cell number availability. Donor 30 was injected with 2 to 10 million cells per mouse, with one mouse, injected with 10 million cells, becoming positive by week 4 post infusion. Similarly, Donor 32 and Donor 34 each had one mouse become positive for viral outgrowth, from 4 and 4.25 million cells, respectively. Donor 42, which was injected with 5 to 7

million cells per mouse, had a total of 3 mice become positive, including the single 7 million cell mouse and two of the 5 million cell mice. Reasonably, the mouse injected with 7 million cells became positive for viremia sooner than those injected with 5 million cells each. This data is consistent with the idea that those mice injected with a larger number of donor cells are more likely to become positive for viral outgrowth. The donor that did not have viral outgrowth by hmVOA, had the least cell viability and poorest health that may have resulted in lack of expansion and activation *in vivo*. In total, these results suggest that the humanized mouse viral outgrowth assay is more sensitive than the gold standard qVOA in detecting latent replication competent virus from systemic donor CD4 T cells that were negative by all other current assays.

Discussion

Continuing advancements in the treatment of HIV-1 have propelled the need for an ultrasensitive method for detection of latent HIV. HIV is capable of going dormant in a variety of cell and tissues reservoirs through a variety of mechanisms, posing an immense challenge concerning complete viral eradication [80]. To date, only one patient, known as the Berlin Patient, has undergone a successful allogenic stem cell transplant with HIV-1 resistant delta 32 CCR5 stem cells. While the qVOA is the gold standard method for detection of replication competent latent HIV-1, it failed to detect latent virus from several other prominent cases, including the Boston patients and Mississippi baby. A number of factors can influence the qVOAs ability to detect low levels of virus [81]. In this regard, a model capable of detecting latent HIV-1 with much higher sensitivity is paramount as the field continues to progress. To address this need, we have developed a highly sensitive model using humanized mice for detection of latent HIV-1 from patient samples that have low to undetectable virus as determined by PCR or qVOA. Humanized mice provide an ideal *in vivo* setting for viral outgrowth as they maintain the cells in a physiological environment for much longer compared to the *in vitro* qVOA, are permissive for HIV-1 infection and permit latent cell reactivation through physiological stimulation.

CD4 T cells isolated from HIV-1 positive donors were subjected to qVOA. The first group of donors, Donor 2 to Donor 15, had successful viral outgrowth by qVOA and thus were used to standardize the hmVOA model. Multiple stimulation methods were tested to determine the optimal approach for viral reactivation and cell viability. A range of cell numbers from each donor were injected in at least duplicate into the humanized mice to determine the minimum number of cells needed to observe viral outgrowth. Thus, a more complete comparison between the humanized mouse viral outgrowth assay and the standard qVOA could be made. To avoid any complication from a single humanized mouse stem cell donor, mice that were generated from different hematopoietic stem cell cohorts were used. Initial experiments examined the likelihood of viral outgrowth for up to 16 weeks. These temporal results concluded that if viral outgrowth was going to occur, it was observed within the first 6 weeks post infusion. If viral outgrowth was not observed up to 8 weeks post infusion, it was not observed over the course of 16 weeks, resulting in all experiments being conducted for only 8 weeks. Based upon this optimization, we were successfully able to achieve viral outgrowth in the humanized mice from all qVOA positive donors. Our sensitivity for lowest number of cells detected matched or improved on the number of cells required for qVOA positivity for donors 2 and 5. Using donor samples 8-15, we continually demonstrated that our model could recapitulate viral outgrowth when the qVOA was positive (Table 3).

To investigate if the hmVOA was more sensitive as compared to the qVOA, we proceed to HIV-1 positive donor CD4 T cell samples that were negative for viral outgrowth by qVOA. Donor CD4 T cells were infused into humanized mice at the largest cells numbers available, as dictated by donor cell number and viability. Due to Poisson distribution of the very rare latent cell population, it is unlikely that all mice infused with donor CD4 T cells will become positive, thus, maximizing cell numbers used to inject increases the likelihood of achieving viral outgrowth. We successfully achieved viral outgrowth in 4 out of the 5 donors used that were negative by qVOA (Table 3). This data suggests that our model is more sensitive for latent viral outgrowth that the current gold standard qVOA.

Table 3 Comparison of hmVOA to qVOA for Viral Outgrowth

Two other studies have modeled the use of immunodeficient mice for the determination of viral outgrowth from HIV-1 latently infected donor cells. The first study used immunodeficient NSG mice that

Donor	qVOA Outgrowth	qVOA IUPM	Lowest # Cells Detected qVOA vs. hmVOA (Millions)	Week of hmVOA Viral Outgrowth
2	+	0.102	5 / 1.25	2
5	+	1.083	1 / 1	3
8	+	4.468	$8x10^{-3}$ / 0.5	2
9	+	1.171	$8x10^{-3}$ / 0.5	1
13	+	3.74	1 / 5	2
15	No data	No data	No Data/ 0.1	1
30	-	0	No outgrowth /10	4
32	-	0	No outgrowth/4	3
34	-	0	No outgrowth/4.25	2
41	-	0	No outgrowth / Not Observed	Not Observed
42	-	0	No outgrowth/5	2

were transplanted with either PBMC or CD4 T cells from 11 HIV-1 positive patients [82]. All the donors used had undetectable viral loads by qRT-PCR, with only a single donor thing negative for viral outgrowth

by qVOA. After infusion of the donor cells into the mice, the mice were systemically administered antihuman CD3 and antihuman CD28 antibodies for increased activation and reduce cytotoxic T cell reaction. Viral outgrowth was successfully observed from all donors used. A study by a different group similarly used immunodeficient NSG that looked into the potential for viral outgrowth from clonal expanded donor derived CD4 T cells [83]. Viral outgrowth was successfully detected from the clonal expanded CD4 T cells that were negative for viral outgrowth by the qVOA.

Whereas the previous studies either require expensive systemic administration of antihuman CD3 and antihuman CD2 8 antibodies, or the costly and time-consuming manipulation of *in vitro* cultured CD4 T cells, the humanized mouse viral outgrowth assay enables long-term stimulation and activation of dormant virus while only necessitating the use of a few million donor cells per injection, with the capability of utilizing a larger number of CD4 T cells than the qVOA when necessary. Humanized mice provide an ideal *in vivo* setting for viral outgrowth as they maintain the cells in a much more physiologically relevant environment in which long-term cell survival and more complete cellular activation can be achieved. Additionally, the hmVOA viral detection for a longer period of time over the standard qVOA, greater than 8 weeks compared to 2 weeks, respectively. This increase in assay duration has been critical in observing viral outgrowth from several donor CD4 T cell samples. As we were highly successfully in obtaining viral outgrowth from patients that were completely negative by qVOA, future directions include the use of donor samples from individuals that have undergone an allogenic stem cell transplant and as well as those patients who are considered elite controllers.

CHAPTER 2

CONDITIONALLY REPLICATING VECTORS FOR MODULATION OF HIV-1 INFECTION IN HUMANIZED MICE

Development of a functional cure for the treatment of HIV-1 is the foremost goal in the field of HIV research. Gene-based strategies represent a promising therapy for the treatment of HIV infection, as they have substantial potential for continued viral inhibition thus reducing the need for daily therapeutic treatment regimens. Conditionally replicating vectors have been explored as such an approach. These vectors are developed to continually express anti-HIV genes in all transduced cells. The vectors then harness HIV- expressed proteins to replicate and spread the therapy within the target cell reservoirs. We have generated and characterized two sets of conditionally replicating vectors for efficacy against HIV-1 infection. The first set of vectors contains shRNA for transcriptional and post-transcriptional inhibition of HIV-1 infection. The second set utilizes CRISPR mediated endonuclease machinery. HIV-1 virus and vector kinetics were monitored in human CD4 T cells as well as *in vivo* in a humanized mouse model generated with vector transduced cells. HIV-1 suppression was observed *in vitro* with the shRNA vectors, with undetectable affects by the CRISPR/Cas9 vectors. Preclinical evaluation into the humanized mouse model provided insight into the feasibility of utilizing genetically modified human CD4 T cells for the modulation of HIV-1 infection. The findings suggest that with additional modifications to the conditionally replicating vector anti-HIV-1 payloads, long-term suppression of HIV-1 using genetically modified patient cells may become a feasible approach in generating a functional cure for HIV-1.

Introduction

HIV-1 has long presented a challenge, as the viral infection that destroys human immune cells currently has no known cure and requires daily drug regimens for modulation of infection. HIV-1 belongs to the lentivirus family, requiring the primary receptor CD4, and either CXCR4 or CCR5 depending on the viral tropism. HIV-1 infection of CD4 T cells is the most widely studied cellular target. Upon binding to CD4 and the required co-receptor, the viral genome undergoes reverse transcription, yielding a DNA

intermediate that is then stably integrated into the host cell genome. This stable integration into the cellular genome results in a significant challenge in the treatment and eradication of the virus. Successful modulation of infection will require a method that can both target HIV-1 specific cellular reservoirs as well as sustain viral inhibition either through transcriptional or post-transcriptional avenues. In this regard, conditionally replicating vectors (CR vectors)utilizing lentiviruses present as a possible approach for the treatment of HIV-1 infection [55, 84-86]. Treatment of HIV-1 target cells with conditionally replicating vectors results in multiple effects against infection via both intracellular and extracellular mechanisms. In addition to modulating the intracellular lifecycle of HIV-1, conditionally replicating vectors are also able to repackage the anti-HIV payload in place of the virulent genome. This competition with production of virulent particles results in the production of a mature virion that targets HIV-1 specific cells and instead delivers anti-HIV-1 payloads (Fig 4).

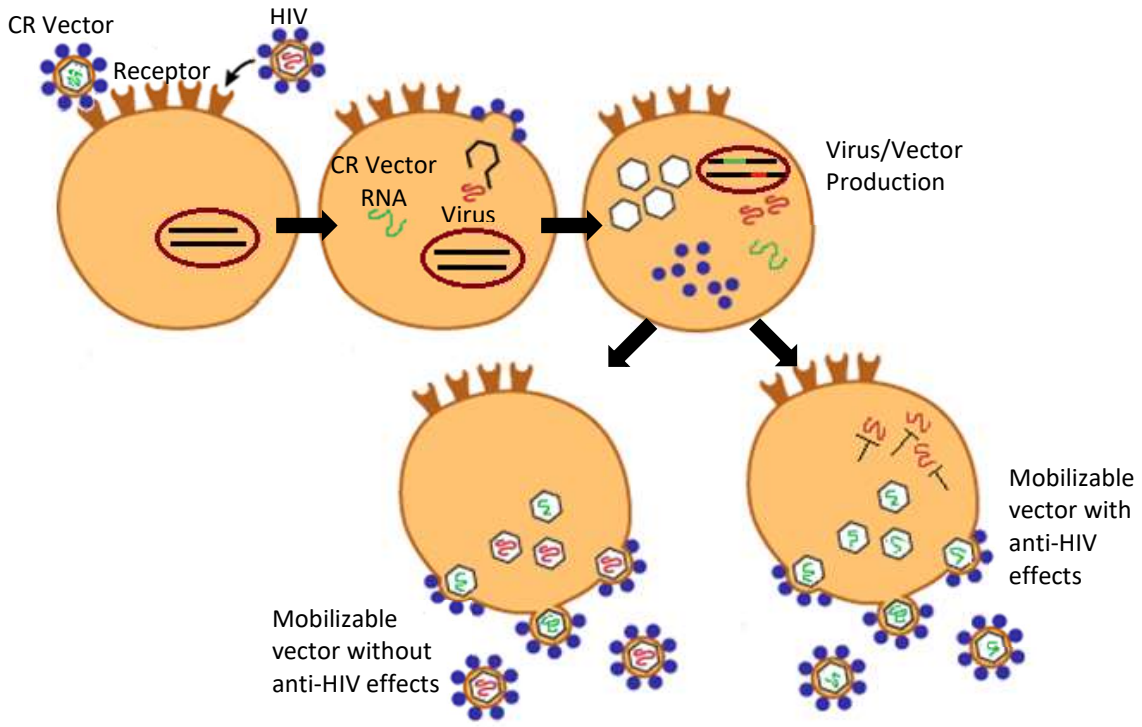

Figure 4 Conditionally Replicating Vector Infection Modulation Schematic. Conditionally replicating vectors stably integrate their anti-HIV payload and when additionally infected by HIV-1, can repackage using HIV-1 packaging proteins to produce mature vectors that can treat other HIV-1 target cells.

Gene therapy utilizing lentiviruses allows therapeutics such as siRNA's and the newly developed CRISPR/Cas system to be stably integrated into an HIV-1 target cell for treatment of infection. As the lentiviral vectors are innately only capable of transducing for a single round, we have harnessed the notion that a vector engineered to pirate HIV specific proteins can act as a conditionally replicating vector capable of spreading mature viral particles that contain the anti-HIV-1 payload. By delivery of small non-coding RNA or CRISPR/Cas genetic cargoes, the vectors are capable of stable integration resulting in expression of anti-HIV-1 machinery that affects the HIV-1 lifecycle through both transcriptional and post-transcriptional modulation [87, 88]. Silencing of HIV-1 with small non-coding RNAs that are trafficked into the nucleus can result in epigenetic silencing of the HIV-1 viral promoter [89]. Modifications of the HIV-1 LTR promoter have been previously demonstrated to be susceptible to transcriptional gene silencing [90, 91]. Additionally, post-transcriptional gene silencing has been an effective gene therapy approach for the treatment of HIV infection. The most notable targets are that of the HIV-1 Tat and Rev transcripts, as these two gene products are required for successful viral genome transcription and regulation of protein expression [48, 92].

In contrast to infection inhibition by lentiviral vector delivery of small interfering RNA, a new tool has been developed for modification of genomic DNA, CRISPR/Cas9. This tool has been examined for efficacy in viral genome silencing and reactivation through epigenetic modifications and complete HIV-1 inhibition through use of Cas9's innate endonuclease activity. This primitive system is quite remarkable as it is highly selective in targeting, with extraordinary ability in DNA manipulation including high efficiency DNA disruption resulting in indel introduction and epigenetic modification. Common delivery for CRISPR/Cas9 is through lentiviral vectors leading to stable integration of the sgRNA and Cas9 construct. Exploration of CRISPR with nuclease deficient Cas9 as an activation tool to reverse latency has shown favorable results as this system is capable of binding to the HIV-1 promoter, recruit transcription factors, and promote viral transcription [93, 94]. A different study, utilizing the excision capabilities, has

demonstrated the ability to stably express the CRISPR/Cas construct in induced pluripotent stem cells that can be efficiently differentiated and maintain resistance to HIV-1 infection [95]. Targeting of host genes, such as CCR5 and CXCR4 that are critical for HIV-1 viral entry, continues to show promise [96, 97]. CRISPR/Cas9 has shown success in editing CXCR4 in primary human CD4 T cells with minimal off-target effects leading to HIV-1 inhibition. HIV-1 viral targets for CRISPR/Cas silencing include the LTR, Gag, Tat, and Rev and have been extensively validated in both immortalized HIV-1 cell lines and primary human cells [98, 99].

Based upon these promising studies, a set of conditionally replicating vectors that encode small non-coding RNAs or CRISPR/Cas9 have been developed for treatment of HIV-1 infection. The conditionally replicating vectors containing small interfering RNA sequences, have been engineered to encode shRNA targeting the HIV-1 LTR promoter, a site previously shown to be susceptible to transcriptional gene silencing, or an shRNA targeting the HIV-1 Tat/Rev transcript, a region that has been shown to be susceptible to RNA silencing through post-transcriptional modification. Similar to the shRNA LTR target, a CRISPR/Cas9 vector targeting the same LTR region has been developed for examination of the CRISPR directed Cas9 excision capabilities for genome disruption. Proof-of-concept studies *in vitro* have revealed that the shRNA vectors are effective at short-term modulation of HIV-1 infection in primary human CD4 T cells, whereas no noticeable repression was seen by the CRISPR/Cas9 vector. Translation into a huPBL humanized mouse model generated by transplantation of conditionally replicating vector modified human CD4 T cells has yielded inconsistent results resulting in the need for further improvement of transduction efficiencies and long-term capacity for anti-HIV effects.

Methods

Vector Production: Six lentiviral-based conditionally replicating vectors were produced (Table 4): pHIV7GFP-IMDH (non-mobilizable GFP only control vector), pMoΔ362.IMDPH.GFP (mobilizable GFP only control vector), pΔ362.Cas.2A.GFP.H1gRNA.CTR (Cas9 control vector with non-specific sgRNA),

pΔ362.Cas.2A.GFP.H1gRNA.F2-362 (Cas9 with sgRNA targeting HIV 5' LTR amino acid position 362), pMoΔ362.IMDPH.GFP-sh362 (shRNA targeting HIV 5' LTR 362 amino acid position 362), and pMoΔ362.IMDPH.GFP-shTat/Rev (shRNA targeting HIV Tat/rev). Vector used for initial validation were supplied by Lentigen and titered by qPCR of integrated vector. Subsequent experiments utilized vectors that were produced from large-scale preparations as previously described [100]. Briefly, using a 3rd generation lentiviral vector system, two packaging plasmids, a VSV-G encoding viral envelope plasmid, and the conditionally replicating vector construct were transfected into HEK 293T cells. Supernatant was collected and concentrated by ultracentrifugation. The vectors were titered by flow cytometry of GFP expression on HEK 293 T cells to determine functional infectious units. Vectors were stored at -80°C.

Table 4 Conditionally Replicating Vector Constructs

Vector Name	Vector Abbreviation	Vector Payload
pHIV7GFP-IMDH	pHIV7	Non-mobilizable GFP vector
pMoΔ362.IMDPH.GFP	pMoGFP	Mobilizable GFP vector
pMoΔ362.IMDPH.GFP-shTat/Rev	shTat	Mobilizable GFP containing shRNA against Tat/Rev
pMoΔ362.IMDPH.GFP-sh362	sh362	Mobilizable GFP containing shRNA against LTR
pΔ362.Cas.2A.GFP.H1gRNA.CTR	CasCTR	Mobilizable GFP vector containing non-targeted CRISPR
pΔ362.Cas.2A.GFP.H1gRNA.F2-362	Cas362	Mobilizable GFP vector containing CRISPR against LTR

Isolation and transduction of human CD4 T cells: Peripheral blood mononuclear cells were isolated from human donor leukopacks using the Ficoll density gradient method following manufacturers suggested protocol. CD4 T cells were isolated by positive selection using CD4 microbeads for magnetic

selection following manufacturers suggested protocol. CD4 T cell purity was greater than 98% as determined by flow cytometry for CD3+/CD4+ cell population. PBMCs and CD4 T cells were cultured in RPMI containing 10% heat inactivated FBS/ 100 units/mL penicillin/ 100 units/mL streptomycin/ 250ng/mL Amphotericin B/ 5ng/mL IL-2. CD4 T cells were activated and expanded using the Miltenyi T cell activation/expansion kit following manufacturers suggested protocol. CD4 T cells were transduced after activation in the presence of 4 µg/mL polybrene at the highest MOI that was achievable for each group of vectors. Transduction efficiency was determined by flow cytometry of GFP positive cells using BD Acurri C6 and analyzed by FloJo Version X.

P24 ELISA for determination of vector anti-HIV efficacy: Anti-HIV activity was determined by amount of P24 capsid protein in cell culture supernatant. Transduced human CD4 T cells were either left uninfected or were infected with HIV-1 NL4-3 at an MOI of 0.001. Cells were cultured in a 96 well plate at 37C and 5% CO2. Cell culture supernatant was collected at day 0, 5, 10, and 15 post infection. Cell culture supernatant from individual wells was collected and purified by centrifugation at 300g for 5 minutes. Supernatant was stored in -80C freezer until analysis by Lenti-X Rapid P24 ELISA kit by Clontech following manufacturers suggested protocol. Plate was read using a Bio-Rad plate reader at 450nm. Statistical analysis was completed by One-way ANOVA.

Vector rescue assay: To determine if the conditionally replicating vectors are mobilizing when in the presence of HIV-1 infection, as would be observed by an increase in CD4 T cell population GFP expression or percentage of transduction of new CD4 T cells with infected

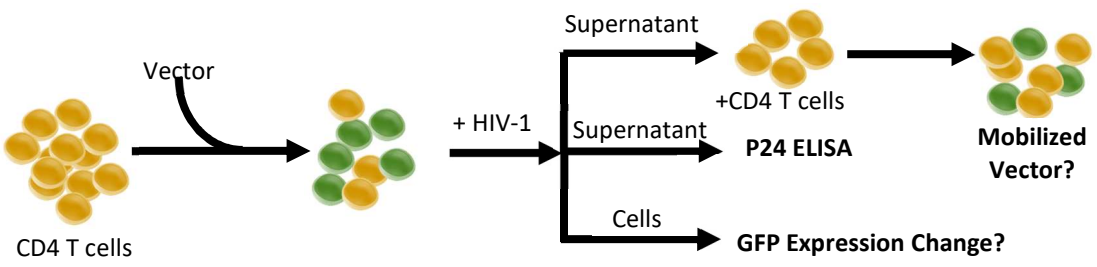

Figure 5 *In vitro* Vector Mobilization and Rescue Assay Schematic. Purified human CD4 T cells were infected transduced with conditionally replicating vector, and then infected with HIV-1. Supernatant was assayed for vector mobilization capacity and IV-1 replication inhibition. Cells were monitored for GFP expression change.

cell culture supernatant, an *in vitro* vector rescue assay was adapted from Evans (Fig 5) [56]. Briefly, human CD4 T cells were transduced with the vectors at the maximum MOI available. Cells were then left uninfected or were infected with NL4-4 at an MOI of 0.001. Cells were cultured in a 96 well plate at 37C and 5% CO2. To determine if the conditionally replicating vectors were spreading *in vitro*, cells were collected at day 0, 5, 10, and 15 post inoculation with HIV-1. Cells were washed once and then fixed with 1% PFA/PBS prior to analysis by flow cytometry. The cells were analyzed by flow cytometry using BD Acurri C6 for determination of GFP levels.

To determine if the conditionally replicating vectors were mobilizing and could be captured in the cell culture supernatant, supernatant from cells that were transduced in either infected or uninfected was collected. The culture supernatant was then used to inoculate allogenic human CD4 T cells. GFP levels were determined by flow cytometry at days 4 and 7 post inoculation using BD Acurri C6 with analysis by FloJo Version X.

Generation of the huPBL humanized mouse model: BALB/c-Rag1$^{null}\gamma c^{null}$ or BALB/c-Rag2$^{null}\gamma c^{null}$ adult mice were used for engraftment with human PBMC and transduced CD4 T cells. Mice were infused intraperitoneally with 1 to 4 million resting PBMC, 1 to 4 million PHA stimulated PBMC, up to 12 million

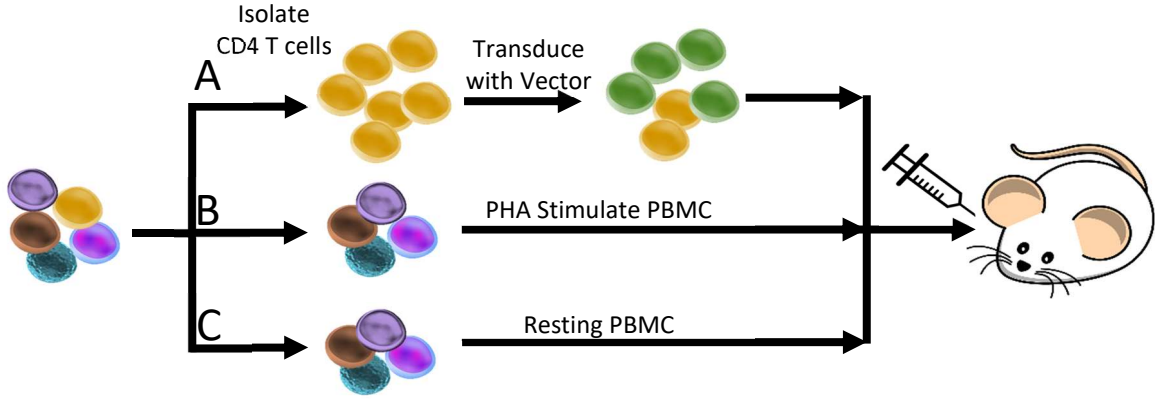

Figure 6 huPBL Generation with Vector Modified Cells A) CD4 T cells are isolated from human donor PBMC, transduced with vector, then infused into adult immunodeficient mice. B) A portion of the remaining PBMC are stimulated with PHA prior to infusion to promote high engraftment levels. C) Remaining resting PBMC are infused into the mice to increase cell diversity.

transduced CD4 T cells, and 1 million transduced CD4 T cells that were infected with NL4-4 at an MOI of 0.01 (Fig 5).

Analysis of human cell engraft in humanized mice: 100 µL of blood was collected via tail vein bleed into EDTA coated tubes. Blood was centrifuged at 350g for 5 minutes. Plasma was removed and blood pellet was resuspended with 100 µL DPBS. 7µl mouse blocking buffer [Normal mouse serum (Jackson Immuno Research Labs), Rat anti-mouse CD16/CD32 (Mouse FC Receptor Monoclonal), Human gamma globulin (Jackson Immuno Research Labs)] was added to each sample, vortexed, and incubated at room temperature for 5-8 minutes. 3µl each of antihuman CD45 APC, CD3 PE, and CD4 PE-Cy7 was added to each sample, vortexed, and incubated for 30 minutes at room temperature in the dark. Samples were lysed and washed following the erythrocyte lysing kit protocol and cells were fixed in 1% paraformaldehyde/DPBS for flow analysis. Samples were ran on the BD Acurri C6 flow cytometer and analyzed by FloJo vX.

HIV-1 viral load determination by qRT-PCR: RNA was extracted from 40 µL of mouse plasma following the Omega E.Z.N.A Viral RNA Extraction kit protocol. RNA was eluted with 50µl DEPC water and stored at -80C. Viral loads were determined by qRT-PCR using iTaq Universal Probes kit with the following a validated protocol adapted from Rouet, HIV-1 LTR Forward Primer -5'GCCTCAATAAAGCTTGCCTTG3' at 500nM, HIV-1 LTR Reverse Primer-5'GGCGCCACTGCTAGAGATTTT3' at 500nM, and HIV-1 LTR Probe-5'FAM/AAGTAGTGTGTGCCCGTCTGT3' at 200nM. Samples were ran using a Bio-Rad C1000 Thermal Cycler with a CFX96 Real-Time System using the following thermocycler protocol: 10 minute 50˚C Reverse Transcriptase step, 3 minute 95˚C Taq activation and DNA denaturation step, 39 cycles of 10 second 95˚C denaturation and 30 second 60˚C anneal/extend/plate read. Viral loads were determined by comparison with an HIV-1 LTR standard curve.

Results

Conditionally replicating vectors containing small interfering RNA repress HIV-1 infection *in vitro*: To validate the anti-HIV effects of the conditionally replicating vectors, human CD4 T cells were transduced with the highest MOI available for each group: pHIV7GFP-IMDH, pMoΔ362.IMDPH.GFP-sh362, pMoΔ362.IMDPH.GFP-shTat/Rev, vectors pMoΔ362.IMDPH. at an MOI of 10, while the pΔ362.Cas.2A.GFP.H1gRNA.CTR and pΔ362.Cas.2A.GFP.H1gRNA.F2-362 vectors were used at an MOI of 2.0. The result in GFP expression levels for those vectors were 76.8%, 18.5%, 3.7%, 25.6%, 1.6% and 1.4%, respectively. These cells were then inoculated with the CXCR4 tropic HIV-1, NL4-3, with supernatant collected at days 0, 5, 10, and 15 post infection. Analysis of the HIV-1 P24 levels by ELISA revealed that

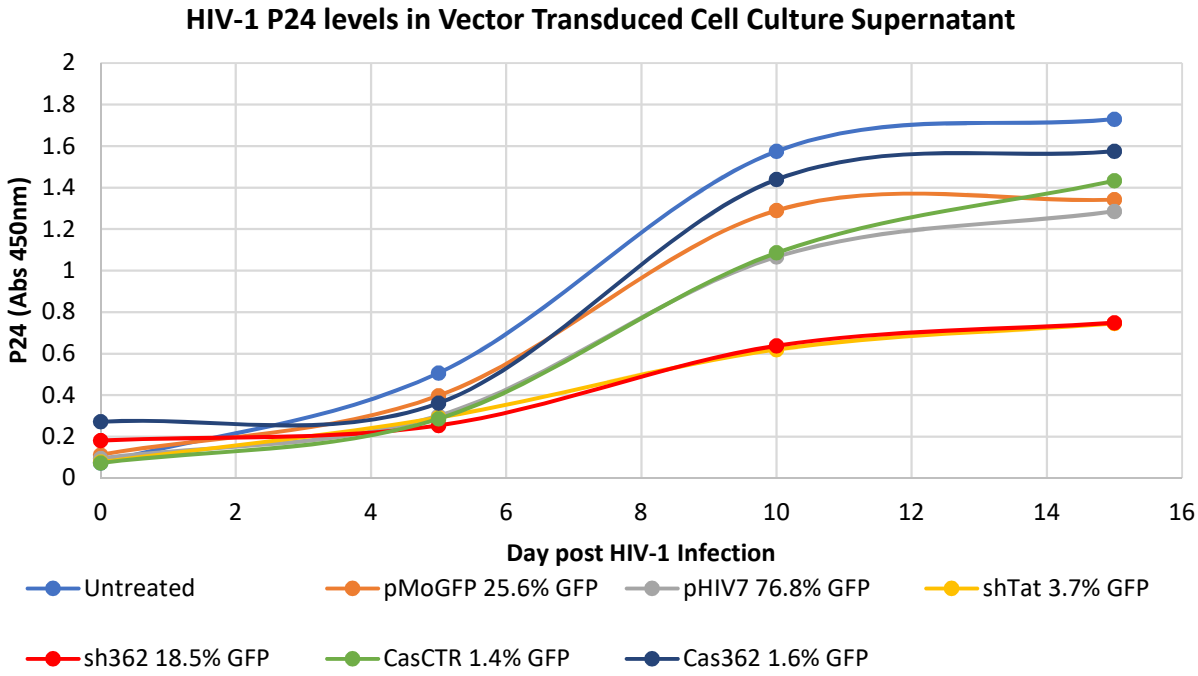

Figure 7 Examination of P24 Levels in Conditionally Replicating Vector Culture Supernatant. CD4 T cells were transduced and the inoculated with HIV-1 at an MOI 0.001. P24 levels were analyzed at days 0, 5, 10, 15 post infection. HIV-1 replication inhibition was observed by both shRNA vectors.

only the shRNA vectors targeting the LTR position 362 and Tat/REV were effective at inhibiting HIV-1 replication over the course of 15 days (Fig 7). In contrast, the CRISPR/Cas construct did not prove to be effective in significantly repressing HIV-1 infection.

Vector mobilization is not observed after HIV-1 infection *in vitro:* Utilizing the cells from the p24 ELISA experiment, vector mobilization capacity was determined by flow cytometry of the percentage of GFP expressing cells. Over the course of the 15 day experiment, there was no change in the percentage of GFP levels (Fig 8).

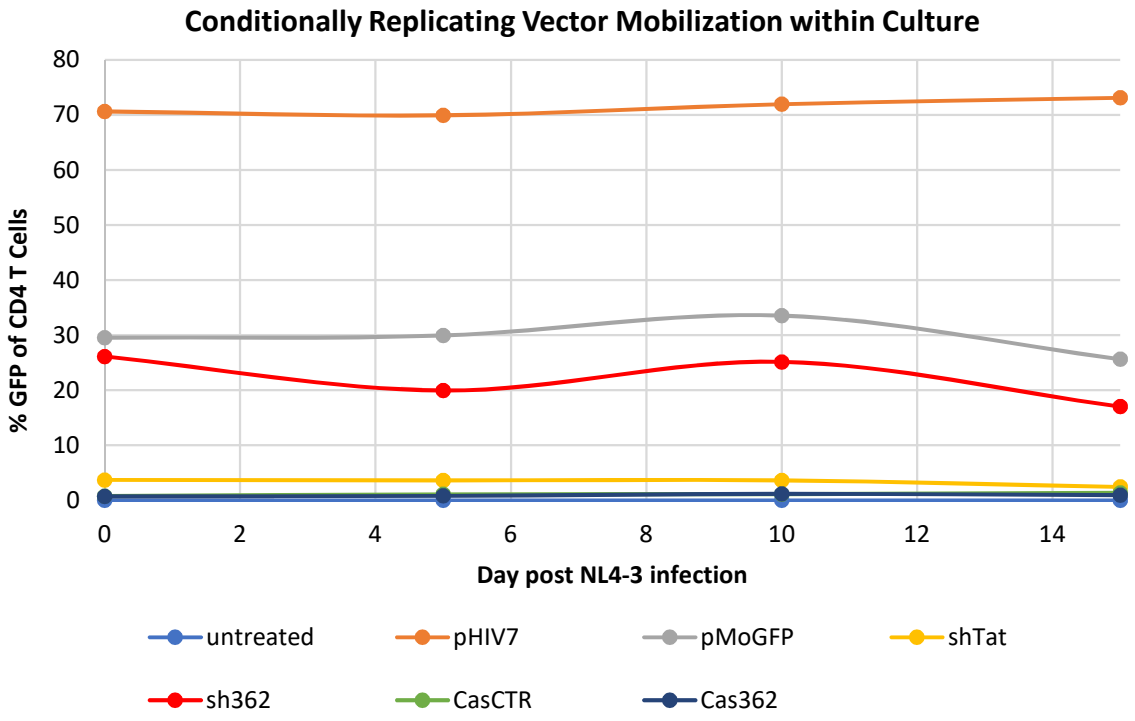

Figure 8 Examination of Conditionally Replicating Vectors to Mobilize within Infected Cell Culture. GFP levels were examined over the course 15 days in conditionally replicating vector transduced cells infected with HIV-1 GFP levels remained stable over the course experiment.

Conditionally replicating vectors cannot be rescued from infected cell culture supernatant: To examine if the conditionally replicating vectors could be mobilized and rescued from the culture supernatant, an *in vitro* mobilization and rescue assay was performed. The objective of the rescue assay was to observe the ability of supernatant from infected transduced cells to generate GFP positive cells in a new culture of untreated CD4 T cells. The same batch of transduced cells that were used in the p24 ELISA experiment were utilized here. Transduced cells were infected with the CXCR4 tropic HIV-1, NL4-3, and incubated for supernatant collection. Clarified supernatant was then inoculated with allogenic CD4 T cells.

The inoculated cells were run on flow cytometry for determination of GFP positive cells that would be indicative of mobilized vector. Surprisingly, no GFP expression was observed in the inoculated cells even after 7 days of incubation. The vectors were unable to harness HIV-1 packaging proteins to mobilize.

Vector	Experiment 1 %GFP	Experiment 2 %GFP	Experiment 3 %GFP
Non-transduced	0.12	0.62	0.09
pHIV7	31.7	76.8	53.6
pMoGFP	5.76	25.7	29.3
shTat	2.3	3.77	6.46
sh362	1.74	18.5	3.67
CasCTR	0.54	1.37	0.84

Cas362	0.15	1.64	0.62

Humanized mice can be generated with conditionally replicating vector modified cells but do not exhibit anti-HIV effects: Three separate *in vivo* experiments were conducted to observe the anti-HIV efficacy of the conditionally replicating vectors. Experiment 1 utilized vectors produced by Lentigen. pHIV7GFP-IMDH, pMoΔ362.IMDPH.GFP-sh362, pMoΔ362.IMDPH.GFP-shTat/Rev, vectors pMoΔ362.IMDPH.GFP were used at an MOI of 4 due to limiting quantities of vector while the pΔ362.Cas.2A.GFP.H1gRNA.CTR and pΔ362.Cas.2A.GFP.H1gRNA.F2-362 vectors were used at an MOI of 1.0 due to low vector titers and limiting quantities, with resultant GFP transduction levels of 31.7%, 1.7%,

Table 5 Conditionally Replicating Vector Transduction Efficiencies Between Each *in vivo* Experiment Demonstrated by Percentage of GFP

2.3%,.7%, 0.5% and 0.1%, respectively (Table 5). Human CD4 T cells were transduced and expanded *in vitro* as previously described.

3 hours prior to infusion into the mice, the CD4 T cells were infected with HIV-1. Eight million transduced infected or uninfected CD4 T cells were infused together with 2 million resting PBMC and 1 million PHA stimulated PBMC. Six mice were used per vector, with 3 mice infected with CXCR4 tropic HIV-1 and 3 mice left uninfected to determine engraftment success.

Mice that were infused with uninfected cells demonstrated consistent levels of engraftment as observed by human CD45 percentage of total mouse lymphocytes (Fig 9A). In these mice, engraftment levels ranged between 5 and 10% CD45 one week post-infusion, with CD45 levels increasing in the untreated, pHIV7GFP-IMDPH, and both shRNA vector transduced cell populations over the course of 4 weeks. The pMoΔ362.IMDPH.GFP and both CRISPR/Cas vector transduced mice had consistent CD45 levels over the course of 4 weeks with mild but not significant decline. All uninfected humanized mice had high levels of CD4 T cells with detectable GFP in the pHIV7GFP-IMDPH remaining between 20 and 30% over the course of 4 weeks (Fig 9B and 9C). The remaining vectors had little to no detectable GFP. Due to the high level of CD45 observed in the humanized mice generated from uninfected transduced CD4 T cells, 5 weeks post infusion the mice were inoculated with CXCR4 tropic HIV-1 to determine if established

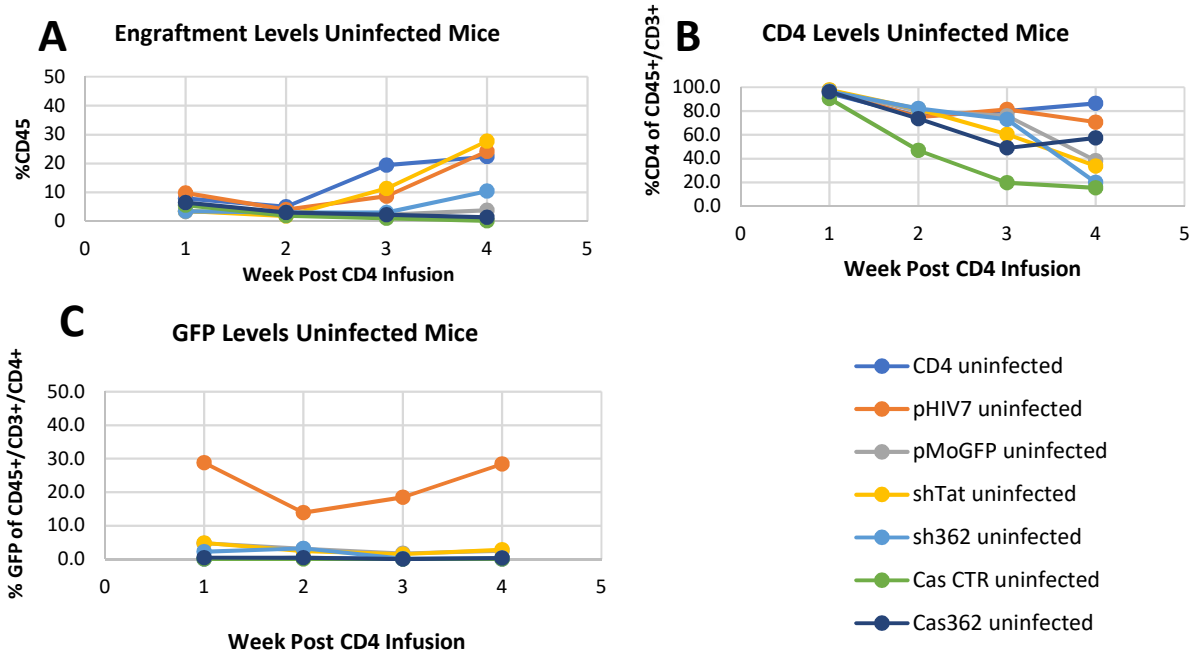

Figure 9 Experiment 1 Uninfected Humanized Mouse Data A) Engraftment levels of uninfected humanized mice as determined by %CD45 of mouse lymphocytes. B) CD4 T cell levels in the humanized mice. C) Circulating GFP levels of the CD4 T cells.

transduced CD4 T cells would be capable of modulating new HIV-1 infection. One week after inoculation, HIV-1 viral loads could be detected in the mouse plasma (Fig 10D). Viral load levels peeked at week 6 and

were undetectable by week 9. This trend is mimicked in both the CD4 T cell and GFP positive population as both populations dramatically declined to nonexistent levels by week 9 (Fig 10A-C).

In contrast, all the mice that had been generated from infected CD4 T cells had between 0.2 and

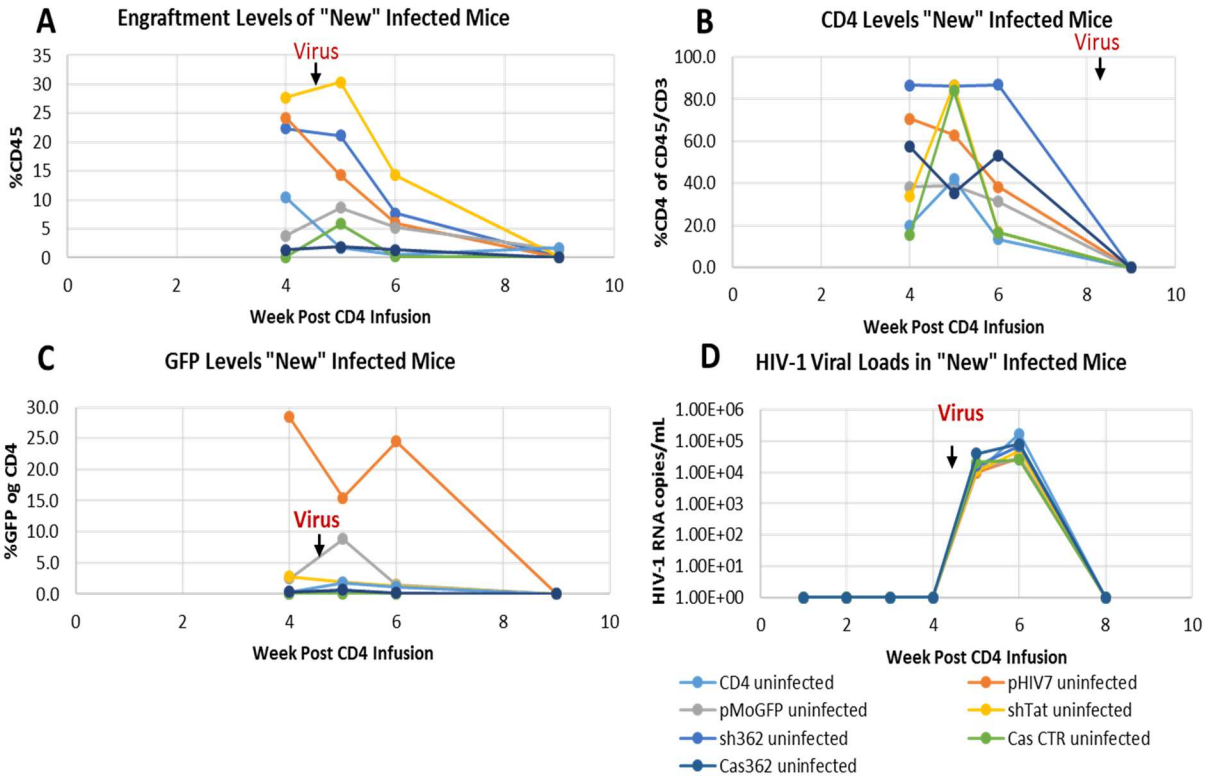

Figure 10 Experiment 1 Infection of Previously Uninfected Mice Mice that were engrafted with uninfected transduced CD4 T cells were challenged with HIV-1 4 weeks post CD4 infusions. A) Engraftment levels humanized mice as determined by %CD45 of mouse lymphocytes. B) CD4 T cell levels in the humanized mice. C) Circulating GFP levels of the CD4 T cells. D) HIV-1 viral load data determined by qRT-PCR of mouse plasma.

0.8% circulating CD45 at week one and week 2 post infusion (Fig 11A). CD4 T cell levels were also substantially declined in comparison to the uninfected mice, with CD4 percentages ranging between 30 and 60% (Fig 11B). GFP was detected at week one post infusion in infected mice that were generated by infusion of the pHIVGFP-IMDPH vector at a similar level to the uninfected mice (Fig 11C). HIV-1 viral loads were also detected at week one post infusion around 1×10^6 HIV-1 RNA copies/mL (Fig 11D). By week 2, GFP levels in HIV-1 viral RNA loads were undetectable. In an effort to salvage the infected humanized mice, additional transduced CD4 T cells were injected 2 weeks post infusion of the initial transduced cells. Week 3 post infusion, a jump in CD45, GFP, and HIV-1 viral load levels was observed. Unfortunately, 2

weeks after injection of additional transduced CD4 T cells, overall CD4 and GFP percentage had rapidly declined, with no detectable HIV-1 RNA copies detectable in the mouse plasma.

In an effort to increase transduction levels of the CD4 T cells, a second *in vivo* experiment was

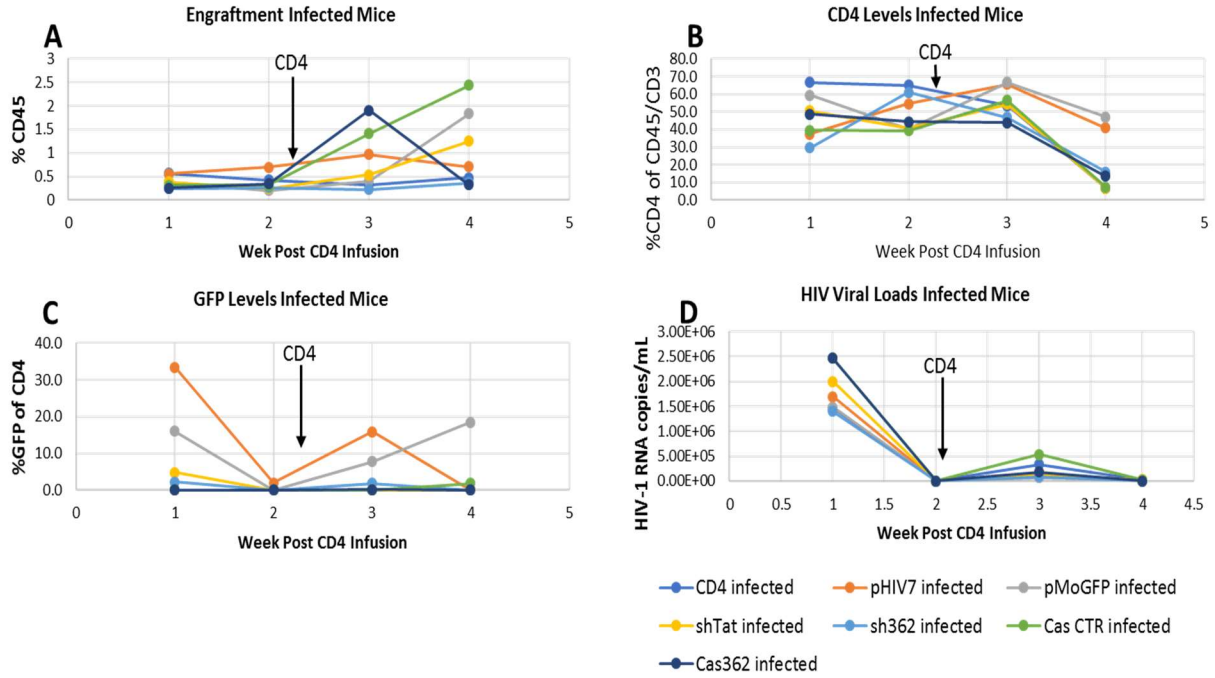

Figure 11 Experiment 1 Infected Humanized Mouse Data Mice were engrafted with HIV-1 infected and vector transduced CD4 T cells. Two weeks post initial engraftment, mice were reinfused with additional transduced CD4 T cells. A) Engraftment levels of infected humanized mice as determined by %CD45 of mouse lymphocytes. B) CD4 T cell levels in the humanized mice. C) Circulating GFP levels of the CD4 T cells. D) HIV-1 viral load data determined by qRT-PCR of mouse plasma.

conducted, Experiment 2. Utilizing vectors that were produced by Lentigen and those produced in lab, pHIV7GFP-IMDH, pMoΔ362.IMDPH.GFP-sh362, pMoΔ362.IMDPH.GFP-shTat/Rev, vectors pMoΔ362.IMDPH.GFP were used at an MOI of 10, while the pΔ362.Cas.2A.GFP.H1gRNA.CTR and pΔ362.Cas.2A.GFP.H1gRNA.F2-362 vectors were used at an MOI of 2.0. The increased MOI resulted in a substantial increase in GFP percentage, with GFP levels of 76.8%, 18.5%, 3.7%, 25.7%, 1.3%, and 1.6%, respectively (Table 5). CD45 levels varied between an average of 10 and 40% depending upon the group (Fig 12A). Low levels of CD4 were detectable in all groups ranging between an average of 10 and 30% (Fig 12B). GFP levels were detectable at week one in the pHIV7GFP-IMDPH and pMoΔ362.IMDPH.GFP, with

all GFP levels substantially dropping off by week 2 (Fig 12C). Unfortunately, by week 2 post infusion while CD45 levels were seen to increase, CD4 T cell levels as well as GFP levels substantially declined. This negative engraftment data resulted in experiment termination as it was unlikely that any repression of HIV-1 infection would be observed due to declining engraftment levels.

The aim of the Experiment 3 was to again target high transduction efficiencies while utilizing a

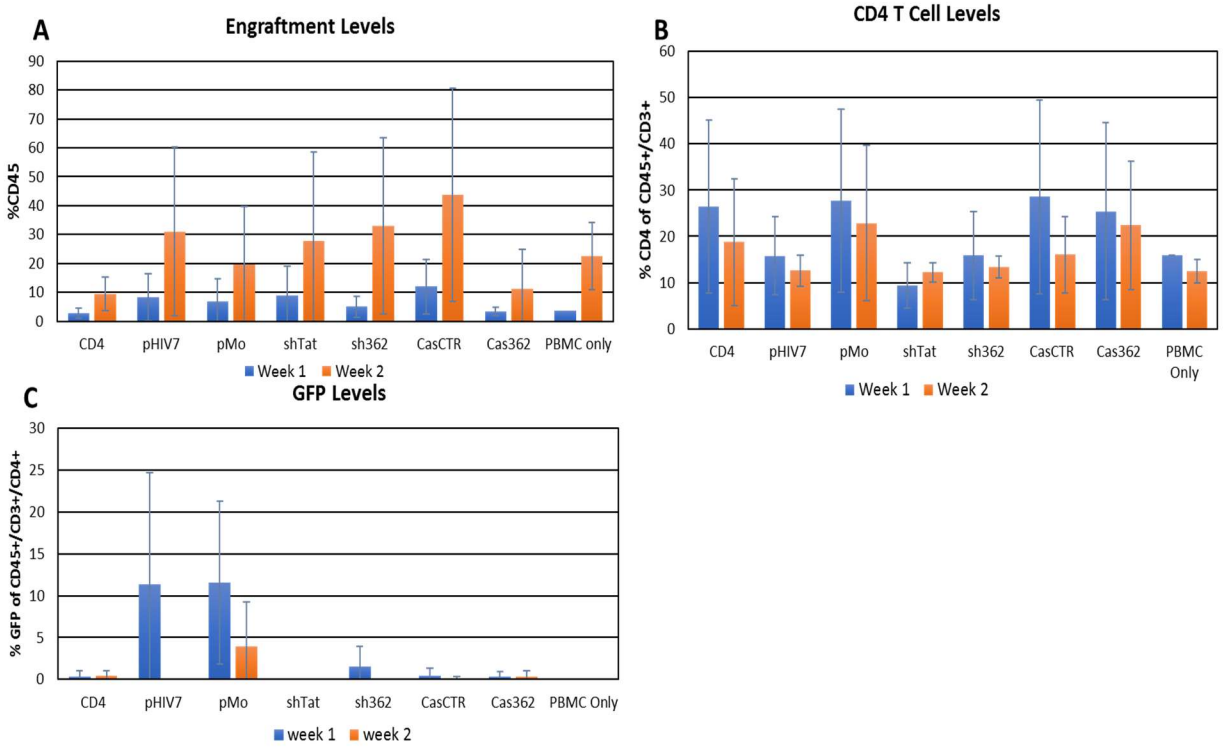

Figure 12 Experiment 2 Humanized Mice Generated from Uninfected Transduced CD4 T cells A) Engraftment levels of humanized mice as determined by %CD45 of mouse lymphocytes. B) CD4 T cell levels in the humanized mice. C) Circulating GFP levels of the CD4 T cells. Error bars represent standard deviation.

different set of donor PBMC and CD4 T cells. Using lab generated conditionally replicating vectors, pHIV7GFP-IMDH was used at an MOI of 10, pMoΔ362.IMDPH.GFP-sh362, pMoΔ362.IMDPH.GFP-shTat/Rev, vectors pMoΔ362.IMDPH.GFP were used at an MOI of 3, while the pΔ362.Cas.2A.GFP.H1gRNA.CTR and pΔ362.Cas.2A.GFP.H1gRNA.F2-362 vectors were used at an MOI of 1.0. Due to the lower MOI as compared to experiment 2, the result in GFP levels of transduced CD4 T cells was 53.6%, 3.6%, 6.4%, 29.3%, 0.8% and 0.62%, respectively (Table 5). All mice were injected with

transduced CD4 T cells along with resting PBMC and PHA stimulated PBMC as before. One week post infusion, all groups had detectable CD45 levels as well as strong CD4 and GFP populations. At this time point, one half of the mice were infused with additional transduced CD4 T cells that were infected with CXCR4 tropic HIV-1. By week 3 post generation of the humanized mice, CD45 levels had declined dramatically along with a steady reduction of CD4 and GFP levels. Altogether, no repression of HIV-1 infection was observed with any of the anti-HIV-1 vectors.

Discussion

Conditionally replicating vectors provide a promising approach for development of a functional cure for treatment of HIV-1. The vectors developed for the study encompass the use of both small non-coding RNAs for transcriptional and post-transcriptional gene silencing as well as the genomic excision capabilities of CRISPR/Cas9.

Conditionally replicating vectors containing small interfering RNA sequences targeting regulation of the well-studied Tat/Rev transcripts as well as a unique position within the LTR were shown to functionally suppress viral replication *in vitro*. In terms of detected p24 levels in culture supernatants transduced with both aptamer-RNAi constructs, almost identical viral inhibition kinetics were observed suggesting that both target sites are similarly as efficient in modulation of viral targets. Consequently, *in vivo* studies revealed that the vector titers were not of a high enough level to adequately transduce a large enough percentage of the CD4 T cell population to be efficacious in inhibiting viral replication. Further investigation into the epigenetic modifications made by the shRNA LTR construct will be needed to elucidate the mechanism and efficiency of transcriptional gene silencing by this construct. The Tat/Rev transcripts has been widely demonstrated as a prime target for inhibition of HIV-1 replication. With further improvement, use of conditionally replicating vectors containing small interfering RNA for gene regulation will enable cells to retain a long-term and highly stable method for post-transcriptional inhibition of viral targets.

Recent developments have brought about the use of CRISPR/Cas as an alternative treatment. Capable of generating an indel or epigenetic modifications, CRISPR/Cas is increasingly progressing as a therapeutic for HIV-1. Once the Cas9 induced double-stranded break is completed, repair is conducted either through NHEJ or HR. Despite the encouraging results, in recent months' new data has arisen shining light on the evidence that HIV-1 can escape the CRISPR/Cas9 attack. Multiple groups recently published information providing possible answers to the unexpected evasion of the CRISPR/Cas9 treatment by HIV-1 infected cells [101-103]. Utilizing cells stably expressing the engineered Cas9/sgRNA construct, with single targets including LTR, gag/pol, or tat/rev, the various groups examined viral inhibition and breakthrough. Although significant viral inhibition was observed during initial culture, viral escape occurred as HIV-1 was able to overcome the Cas9/sgRNA barrier. Further examination revealed that the non-homologous end joining (NHEJ) repair pathway acts as a double-edged sword both introducing lethal indels and surprisingly, generating indels permitting viral resistance. Additional confirmation by another group again suggested that NHEJ repair enables viral adaptation for Cas9/sgRNA evasion, as was demonstrated with their *in vitro* cell models using sgRNA targets for LTR, gag/pol, and tat/rev and sequence analysis of viral mutations. This evasion of the CRISPR/Cas9 system is likely being observed in our conditionally replicating vector studies *in vitro* and in the humanized mouse model. Due to the limited number of transduced cells and rapid ability of HIV-1 viral mutants to overcome selective pressures and sustain viral replication, higher vector titers, more efficient vector transduction, and addition of multiple CRISPR targets will be required to reduce the number of viral escape mutants.

Further investigation into the utility of the conditionally replicating vectors as a gene therapy method for HIV-1 infection will need to be completed to suggest that these vectors will be a viable method for long term stable regulation of HIV infection in the absence of antiretroviral drugs.

CHAPTER 3

APTAMER siRNA CONJUGATES FOR TREATMENT OF HIV-1 INFECTION HUMANIZED MICE

The advent of HAART has made instrumental strides towards reducing the HIV/AIDS fatality rates. Though relatively normal long-term lives are led by patients on such treatment, a cure has yet to be discovered. Such long-term drug treatments have led to drug toxicity and generation of viral mutants that present problems during therapy. Thus, novel anti-viral molecules are in need. In this regard, alternative drug therapies using aptamers for modulation of HIV-1 infection are being explored and are showing considerable promise. Therefore, an RNA-based aptamer with high binding affinity to HIV-1 gp120 viral envelope protein has been conjugated to a small interfering RNA that triggers sequence specific degradation of HIV-1 transcripts. The aptamer conjugate is capable of virus neutralization with the advantage of siRNA payloads delivery only to those cells demonstrating infection as observed through virus budding. Two siRNA sequences were studied, including one targeting the HIV-1 LTR promoter for transcriptional gene silencing and the second siRNA sequence targeting the HIV-1 Tat/Rev transcripts for post-transcriptional gene silencing. Our initial study focused on treatment of humanized mice infected with CXCR4 tropic HIV-1, with subsequent studies investigating the aptamer conjugates viral suppression efficacy in primary human CD4 T cells against both CXCR4 and CCR5 tropic HIV-1 *in vitro*. The *in vitro* results led to a small pilot study to investigate the aptamer siRNA conjugate efficacy against CCR5 tropic HIV-1 infection in humanized mice. Overall, the results suggest that the aptamer is CCR5 virus specific with both siRNA sequences effectively repressing HIV-1 replication *in vitro*. Further investigation into aptamer siRNA stability *in vivo* is necessary.

Introduction

Stable HIV genome integration into the hosts' cell chromosome and predilection for establishing latency pose large challenges for the development of a complete cure. The development and administration of highly active antiretroviral therapy (HAART) targeting various stages of viral replication

are now routinely given to HIV-1 infected patients leading to sustained reduction and suppression in viral loads and conserved CD4 cell levels. Combining up to three antiretroviral drugs, the progression to AIDS has been highly diminished resulting in HIV-1 infection acting no longer as a death sentence. However, complete virus eradication with HAART does not exist as HIV-1 is able to persist in a latent state unperturbed by these current therapies. As a consequence, indefinite treatment is required resting highly on a patients adherence to the regimen. In this regard, innovative forms of treatment, such as aptamer's and RNAi, are being explored to minimalize toxicity, increase efficacy, and act as a functional cure.

RNA-based antiviral constructs are encouraging replacements to current drug therapies due to their novel mechanisms of action and reduced immunogenicity. RNAi is an enticing approach as it cleaves viral or host transcripts as a means of post transcriptional gene silencing inhibiting viral replication [104, 105]. Development of siRNA approaches for silencing of HIV-1 have been widely reviewed in the last decade with primary targets comprised of highly conserved viral genome regions [106, 107]. Delivery of RNAi treatments pose challenges as current strategies include transient expression or lentiviral vector delivery causing toxicity and immunogenicity resulting in clinical therapeutic limitations for RNAi applications. Recent innovations in genetic engineering technologies enables targeted RNAi therapy using an aptamer based delivery system [108, 109]. Aptamers are constructed from single-stranded nucleic acids that are capable of extremely specific interactions with high affinity. Aptamer's act like antibody like molecules and can both work in virus neutralization or for the delivery of siRNA. Aptamers have been generated against viral targets, like reverse transcriptase (RT) and gp120, or cellular receptors, like CD4 and CCR5 (Fig 13) [44, 49, 110]. Studies expanding on the functionality of aptamers as a means for delivery of anti-HIV constructs have conjugated the aptamer to siRNA molecules targeted to either viral, e.g. Tat/Rev, RT, and env, or cell transcripts, e.g. CCR5 and CXCR4 [47, 48]. CD4 aptamer-siRNA conjugates have further shown to be an effective pre-exposure prophylaxis treatment *in vivo* when prepared as a vaginal microbicide [111]. Most recently, RNA aptamers targeting CCR5 have been developed as aptamer-

siRNA chimeras inhibiting viral replication successfully *in vitro* [44]. Using SELEX technology for rapid determination of CCR5 aptamer constructs, siRNA-aptamer conjugates were designed and demonstrated cell-specific internalization and functional HIV-1 inhibition.

Anti-gp120 aptamers have been effective at delivering anti-HIV siRNAs with improved stability and efficacy. Enhanced aptamer modifications include noncovalent binding of aptamer to siRNA via sticky bridge. This group of *in vitro* transcribed aptamer-siRNA conjugates was shown to be effective at complete suppression of HIV-1 viral loads in humanized mice [48]. Expanding on this previous research, we have

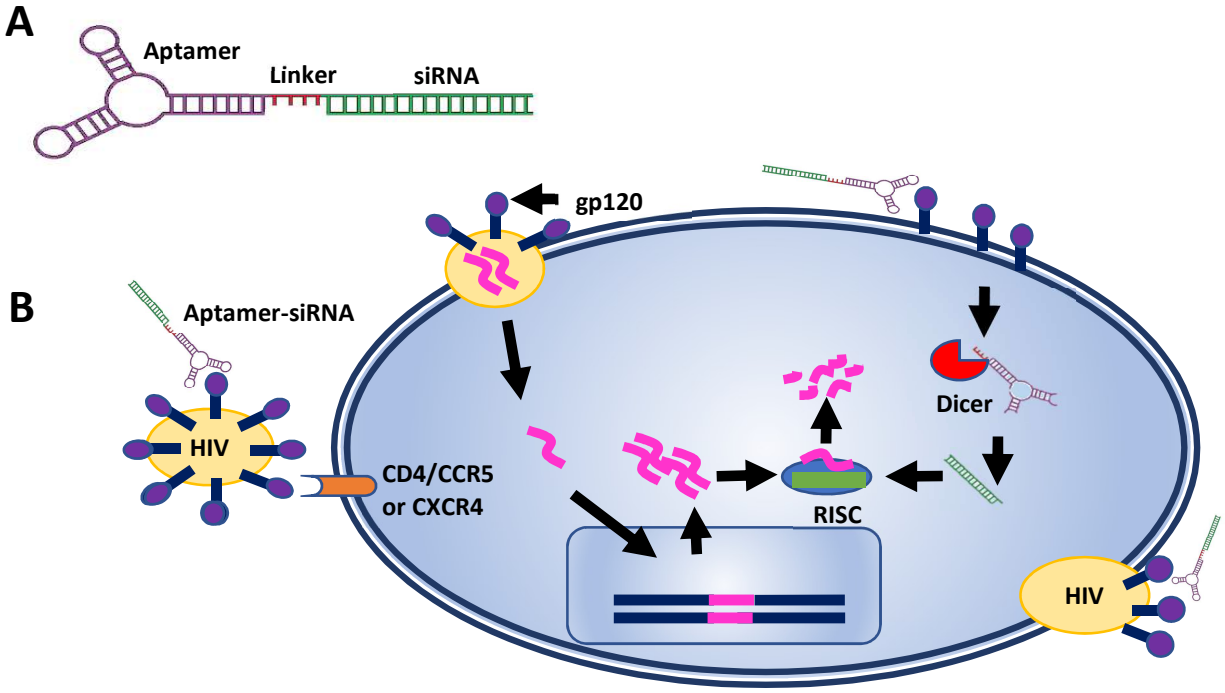

Figure 13 Aptamer Conjugate Function Schematic A) Primary structure of aptamer plus siRNA. B) Interaction of aptamer conjugate for virus neutralization and delivery of siRNA into cell for transcriptional and post-transcriptional gene silencing. Aptamer-siRNA conjugates can interact with mature virions for virus neutralization, or interact with gp120 on the cell membrane and undergo siRNA interference.

developed new aptamer-siRNA conjugates utilizing this previously validated anti-gp120 RNA aptamer construct. The anti-gp120 aptamer construct was chemically synthesized and conjugated to a novel siRNA targeting HIV-1 LTR. The aptamer siRNA targeting the LTR was investigated for anti-HIV efficacy in comparison to the previously validated aptamer siRNA targeting Tat/Rev in a humanized BALB/c-Rag1$^{null}\gamma c^{null}$ or BALB/c-Rag2$^{null}\gamma c^{null}$ mouse model engrafted with human CD34 hematopoietic stem cells

capable of multilineage human hematopoiesis as well as *in vitro* utilizing primary human CD4 T cells. The anti-HIV efficacy of the aptamer conjugates was initially determined against CXCR4 tropic HIV-1 in humanized mice, with further studies investigating the aptamer viral tropism specificity and anti-HIV efficacy against CXCR4 and CCR5 tropic HIV-1.

Methods

Aptamer synthesis: Anti-HIV gp120 aptamer sequence as previously published, was used, with siRNA groups containing either a nonspecific siRNA, a Tat/Rev siRNA, or an LTR siRNA. RNA sequences for the aptamer and siRNA were chemically synthesized. Aptamer, forward sense siRNA and antisense siRNA oligonucleotides were annealed together within 72 hours prior to injection into humanized mice, and stored at -80°C and until injection. The conjugated aptamers were thawed and diluted with nuclease free phosphate buffered saline such that each dose contained 1 nMol.

Preparation of humanized mice: BALB/c-Rag1$^{null}\gamma c^{null}$ or BALB/c-Rag2$^{null}\gamma c^{null}$ 1-4 day old neonates were irradiated at a non-lethal dose of 3.5 gy up to 24 hours prior to engraftment. Pups were injected intraheptatically with 0.3-1.0x10^6 CD34 human hematopoietic stem cells. 12 weeks after injection, 50 µL of blood was collected via tail vein bleed with heparin treated tubes. As previously described, mice were screened for engraftment by the presence of human CD45 the pan human leukocyte marker, CD3 T cells, and CD4 T helper cells as determined by flow cytometry using BD Accuri C6 and analyzed by FloJo vX.

HIV-1 infection and aptamer conjugate administration in humanized mice: Humanized mice used for this study were infected with CXCR4 or CCR5 tropic HIV-1, NL4-3 or Bal, respectively, depending upon the experiment. Mice were inoculated with 200 µL of stock virus administered by intraperitoneal injection. Mice demonstrated consistent infection for a minimum of 4 weeks prior to treatment. Aptamer-siRNA was diluted such that 50µl injection per mouse was equivalent to 1nMol of aptamer conjugate. Treatment was administered by intravenous injection weekly for 6 weeks. Blood and plasma samples were collected weekly for determination of CD4 T cell engraftment levels and HIV-1 viral load levels.

The pilot study used Bal infected humanized mice that had demonstrated continual viral loads for 6 weeks prior to aptamer injection. 0.5 nMols of aptamer conjugates were administered per injection. Mice were injected at day one, 2, and 8. Plasma was collected by tail vein bleed at day zero, 5, and 12 post initial aptamer injection for viral load determination.

Human cell engraftment analysis of humanized mice: Two capillaries of blood were collected via tail vein bleed into EDTA coated tube. 90µl DPBS was added to each tube and mixed. Blood was centrifuged at 350g for 5 minutes. 150µl plasma was transferred to new labeled 1.5ml tube and stored at -80C. Blood pellet was resuspended with 100µl DPBS. 7µl mouse blocking buffer [Normal mouse serum (Jackson Immuno Research Labs), Rat anti-mouse CD16/CD32 (Mouse FC Receptor Monoclonal), Human gamma globulin (Jackson Immuno Research Labs)] was added to each sample, vortexed, and incubated at room temperature for 5-8 minutes. 3µl each of antihuman CD45 FITC, CD3 PE, and CD4 PE-Cy5 was added to each sample, vortexed, and incubated for 30 minutes at room temperature in the dark. Samples were lysed and washed following the Erythrocyte lysing kit protocol and cells were fixed in 1% paraformaldehyde/DPBS for flow analysis. Samples were ran on the BD Acurri C6 flow cytometer and analyzed by FloJo vX.

HIV-1 viral loads by qRT-PCR analysis: Two capillaries of blood were collected via tail vein bleed into EDTA coated tube. 90µl DPBS was added to each tube and mixed. Blood was centrifuged at 350g for 5 minutes. 150µl plasma was transferred to new labeled 1.5ml tube and stored at -80C until RNA extraction. Plasma was thawed and brought to room temperature prior to RNA extraction. RNA was extracted following the Omega E.Z.N.A Viral RNA Extraction kit protocol. RNA was eluted with 50µl DEPC water and stored at -80C.

Viral loads, for both NL4-3 and Bal HIV-1 virus strains, were determined by qRT-PCR using iTaq Universal Probes kit with a validated protocol adapted from a publication by Rouet: HIV-1 LTR Forward Primer -5'GCCTCAATAAAGCTTGCCTTG3' at 500nM, HIV-1 LTR Reverse Primer-

5’GGCGCCACTGCTAGAGATTTT3’ at 500nM, and HIV-1 LTR Probe-5’FAM/AAGTAGTGTGTGCCCGTCTGT3’ at 200nM. Samples were ran using a Bio-Rad C1000 Thermal Cycler with a CFX96 Real-Time System using the following thermocycler protocol: 10 minute 50˚C Reverse Transcriptase step, 3 minute 95˚C Taq activation and DNA denaturation step, 39 cycles of 10 second 95˚C denaturation and 30 second 60˚C anneal/extend/plate read. Viral loads were determined by comparison with an HIV-1 LTR standard curve.

ELISA for HIV-1 P24 capsid protein: Primary human CD4 T cells were infected with NL4-3 or Bal at an MOI 0.001. 3 days post infection, cells were washed three times with PBS and cultured in complete media containing 400nM aptamer, as previously published. Culture supernatants were collected at day 3,5,7,9, and 11 days post aptamer exposure. All treatments were done in triplicate. Supernatant samples were frozen at -80C until analysis. P24 levels in culture supernatant were analyzed by Lenti-X Rapid P24 ELISA kit from Clonetech following manufacturers suggested protocol. Plate was read using a Bio-Rad plate reader with absorption 450nm. Statistical analysis was done by One-way ANOVA.

Sanger sequencing for HIV-1 viral stock tropism verification: Sanger sequencing of lab stocks of NL4-3 and Bal that were used in the various experiments were completed to confirm HIV-1 strain sequence identity. Briefly, viral stock RNA was isolated following OMEGA E.Z.N.A Viral RNA extraction kit protocol. PCR amplification targeting a 500bp region of the V3 loop of gp120, sequence known to define strain tropism, using Invitrogen SuperScript One-Step with Platinum Taq was completed. PCR products were purified by magnetic bead cleanup using ChargeSwitch PCR Clean-Up kit following manufacturers suggested protocol. Multiple Sanger Sequencing primers were developed and used for sequencing of viral stocks. Samples were sent for sequencing to Genewiz. Chromatograms were received and analyzed for accuracy of base call. Sequences were then ran on NIH BLAST for alignment and sequence identity.

Results

Aptamer siRNA conjugates were ineffective in suppressing HIV-1 viral loads in CXCR4 tropic HIV-1 infected humanized mice: Mice were infected for 6 weeks with NL4-3 as demonstrated by qRT-PCR of mouse plasma. Mice were broken up into 5 groups of 4 mice each: uninfected, infected untreated, infected treated with aptamer non-specific siRNA (A-1 scramble), infected aptamer siRNA Tat/Rev (A-1 Tat/Rev), and aptamer siRNA LTR (A-1 LTR). Mice were injected weekly with aptamer conjugates for 6 weeks, starting at week 7 post infection. Mice were monitored for a total of 13 weeks. There was no anti-HIV effect by the aptamer constructs on HIV-1 viral loads (Fig 14A). Viral load levels remained consistent with no statistical difference between treatment and control groups. Additionally, CD4 T cell levels steadily declined in all infected groups, with no T cell conservation or recovery observed in either the A1-LTR or A1-Tat/Rev treatment groups (Fig 14B). Infected aptamer treated and infected control mice display a continual downward trend of CD4 T cells levels, consistent with productive HIV-1 infection. The uninfected mice maintained steady CD4 T cell levels throughout the experiment.

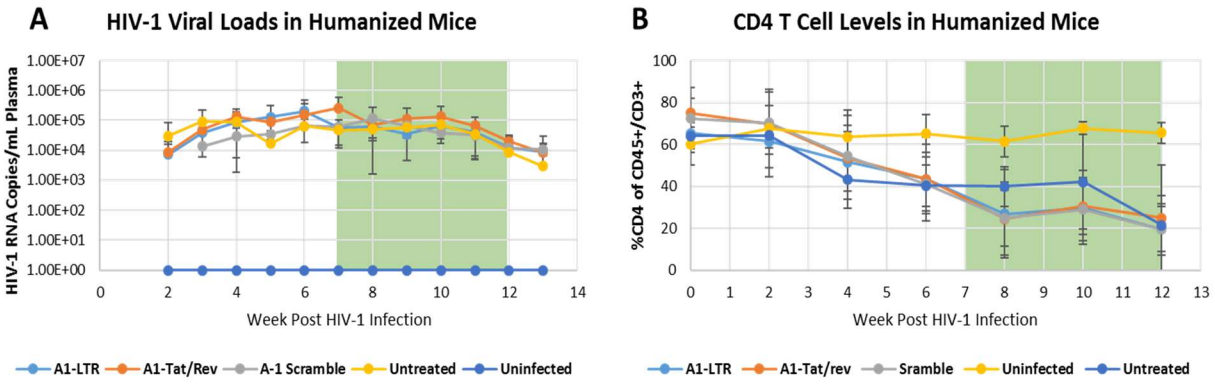

Figure 14 Aptamer Conjugate Treatment of Humanized Mice A) CD4 level averages in mice uninfected, infected and left untreated, or infected and treated with aptamer. B) HIV-1 viral load averages in mice treated with each aptamer, infected and left untreated, or uninfected. Shaded portion represents aptamer treatment period. Error bars represent standard deviation.

Anti-HIV aptamer conjugates are efficacious in repressing HIV-1 infection against CCR5 tropic HIV-1 *in vitro*: To determine if aptamer conjugates were effective at suppressing HIV-1 replication, an *in vitro* assay was conducted as previously described using the aptamer conjugates that were remaining from the first *in vivo* experiment. Briefly, human primary CD4 T cells were infected with CXCR4 or CCR5 tropic HIV-1 and then subjected to aptamer treatment in culture. HIV-1 p24 capsid protein levels were quantified by ELISA and treatment groups were compared to infected untreated cells. The A-1 Tat/Rev and the A-1 LTR constructs significantly reduced the p24 levels in the CCR5 infected cultures, with no anti-HIV effects observed A-1 scramble group (Fig 15A-B). There was no effect on p24 levels in any of the aptamer treated groups in the CXCR4 infected cells.

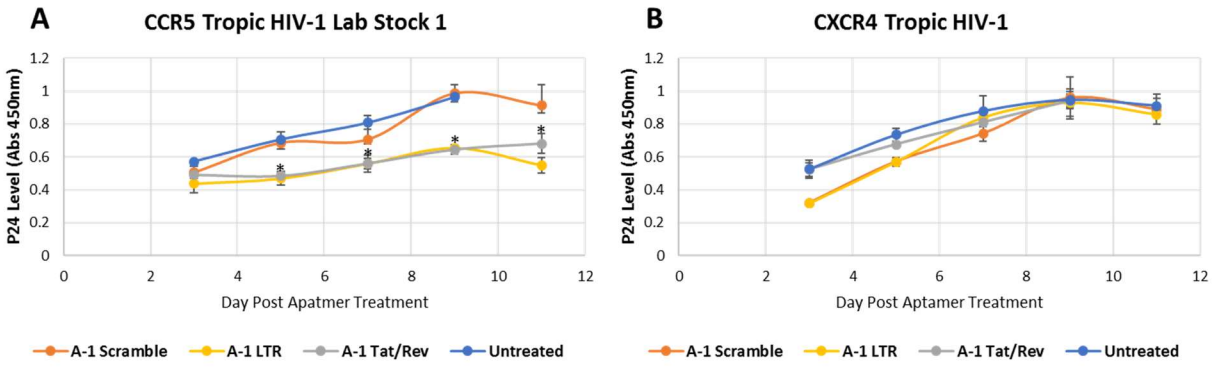

Figure 15 Experiment 1 *in vitro* Determination of Aptamer Conjugate Efficacy A) CD4 T cells infected with CCR5 tropic HIV-1, Bal, virus at MOI=0.001. Following infection, cells were treated with media containing 400nM aptamers: A-1 scramble, A-1 LTR, A-1 Tat/rev, or left untreated. * $p<0.05$ B) CD4 T cells infected with CXCR4 tropic HIV-1, NL4-3, virus at MOI=0.001. Following infection, cells were treated with media containing 400nM aptamers: A-1 scramble, A-1 LTR, A-1 Tat/rev, or left untreated. Statistical analysis by One-Way ANOVA

To confirm these results, a second *in vitro* aptamer efficacy assay was performed (Fig 16A-C). An additional stock of CXCR4 tropic HIV-1 produced from a second lab was used in addition to the previous CXCR4 tropic HIV-1 stock and CCR5 tropic HIV-1 virus stocks to infect primary CD4 T cells. Sanger sequencing confirmed 100% sequence identity of both viral stocks to that of NIH accession number U26942.1 and AB 521136.1, respectively. Confirming the previous results, HIV repression was observed in the CCR5 tropic HIV-1 infected CD4 T cells that were treated with the A-1 Tat/Rev, A-1 LTR, and additionally

the A-1 scramble. No statistically significant suppression in the p24 levels of the CXCR4 tropic HIV-1 infected CD4 T cells that were incubated with any of the aptamer's existed.

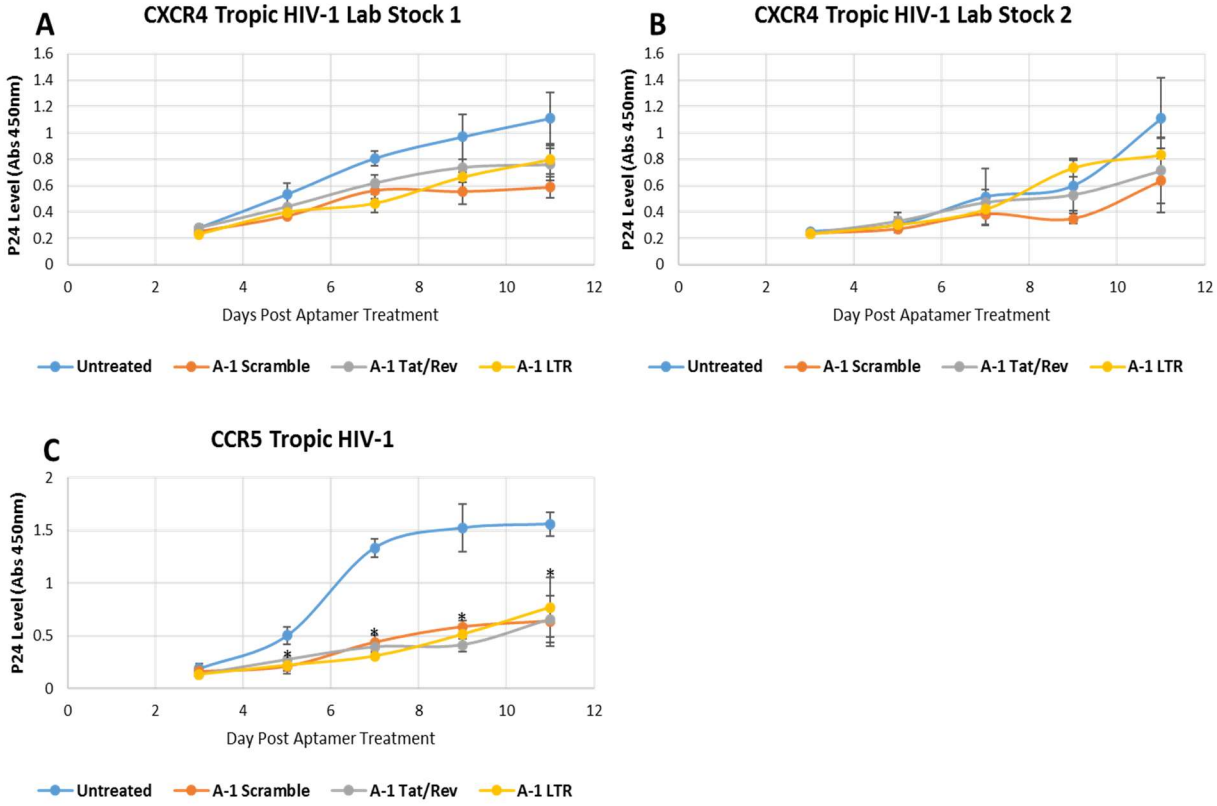

Figure 16 Experiment 2 *in vitro* Determination of Aptamer Conjugate A) CD4 T cells infected with CXCR4 tropic HIV-1, NL4-3, lab stock 1. B) CD4 T cells infected with CXCR4 tropic HIV-1, NL4-3, lab stock 2. C) CD4 T cells infected with CCR5 tropic HIV-1, Bal, virus. Following infection, cells were treated with media containing 400nM aptamers: A-1 scramble, A-1 LTR, A-1 Tat/rev, or left untreated. * $p<0.05$ Statistical analysis by One-Way ANOVA

Aptamer conjugate treatment of CCR5 tropic HIV-1 infected humanized mice failed to suppress viral loads in a pilot study: CCR5 tropic HIV-1 infected humanized mice were administered a total of 3 doses of 0.5 nMols aptamer conjugates by intravenous injection. No anti-HIV activity was observed as seen by steady viral load levels throughout the course of the experiment (Fig 17).

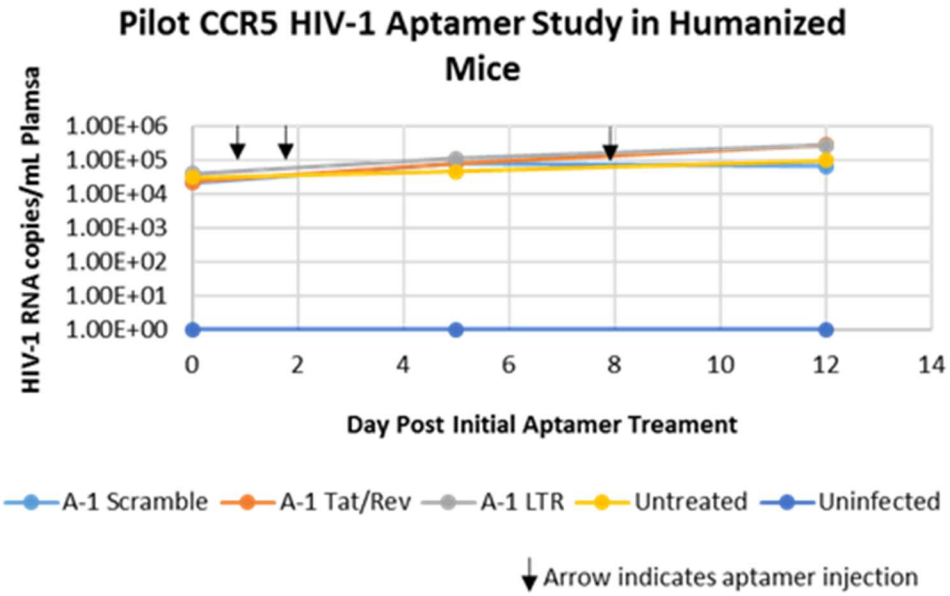

Figure 17 Pilot Aptamer-siRNA Conjugate Experiment Using CCR5 Tropic HIV-1 Infected Humanized Mice. Mice were infected with CCR5 tropic HIV-1 and then treated with aptamer-siRNA conjugates.

Discussion

With valuable use as a means of delivery for RNAi, aptamers offer promise for surmounting current therapeutic delivery challenges. Aptamers-siRNA chimeras display reduced immunogenicity, desired pharmacokinetic stability and can work as both a neutralizing antibody like molecule as well as deliver potent RNAi. Previous *in vitro* and *in vivo* validation studies have demonstrated the effectiveness of HIV-1 anti-gp120 aptamer's in successfully suppressing HIV-1 viral loads [48]. In humanized mice infected with CXCR4 tropic HIV-1, intravenous aptamer administration dramatically reduced HIV-1 viral loads within one week of injection and demonstrated CD4 T cell conservation over the course of the treatment. The study further investigated the use of the anti-gp120 aptamer to deliver and siRNA payload targeting the HIV-1 Tat/Rev. The results showed success with 0.25 nMols of either aptamer or aptamer conjugates in suppression of CXCR4 tropic HIV-1 viral loads within one week of administration and for the duration of treatment.

To build on the study, the anti-gp120 aptamer was chemically synthesized, and utilizing a sticky bridge linker, was conjugated to the previously successful Tat/Rev siRNA as well as a novel siRNA targeting the HIV-1 LTR position 362. The LTR 362 target site is a region with in the 5' LTR locus that contains a unique NF-κB doublet that has been observed to be highly susceptible to transcriptional gene silencing via RNAi. Surprisingly, neither the previously validated aptamer or the novel new aptamer-siRNA conjugate showed any efficacy in HIV-1 viral suppression in CXCR4 tropic HIV-1 infected humanized mice.

Due to the negative data collected in humanized mice infected with CXCR4 tropic HIV-1, the functionality of the aptamer siRNA conjugates was determined against both CXCR4 and CCR5 tropic HIV-1 infected human CD4 T cells. Surprisingly no repression of CXCR4 HIV-1 p24 capsid levels was observed with any of the therapeutic aptamer conjugates, suggesting that the aptamer's sequence and tertiary structure is not conducive for binding to CXCR4 tropic HIV-1. Furthermore, significant anti-HIV effects were observed by both the A-1 Tat/Rev and the A-1 LTR treated cells in the CCR5 tropic HIV-1 infected cell cultures. While aptamers are known to act in an antibody like manner capable of viral neutralization, this effect was not apparent as the aptamer conjugated to a scrambled siRNA did not show any viral suppression. Thus this initial viral inhibition is likely do to siRNA mediated gene silencing.

In an effort to confirm the aptamer functionality, an additional stock of CXCR4 tropic HIV-1 virus from the lab that initially validated the aptamer conjugates was used to repeat the *in vitro* assay. Freshly conjugated aptamer-siRNA conjugates were used for the second *in vitro* experiment to determine if long-term storage at -80°C led to degradation of the RNA aptamer. Confirming the previous results, the A-1 Tat/Rev and A-1 LTR significantly suppressed p24 levels in the CCR5 tropic HIV-1 infected CD4 T cell culture. Additionally, viral suppression was also observed in the A-1 scramble group, likely resulting from direct aptamer inhibition of mature virions. No significant viral suppression was observed in either of the CXCR4 tropic HIV-1 infected cultures. Altogether, the two *in vitro* assays demonstrate the anti-HIV efficacy of the therapeutic siRNA's, as well as the ability of the anti-gp120 aptamer to neutralize CCR5 tropic HIV-

1 virus when fresh aptamer stocks are used. As both viral stocks mapped to 100% sequence identity of their known tropic genome sequence, it is likely that the aptamer specificity is to that of CCR5 tropic HIV-1 rather than genetic drift of the viral stocks used for infection affecting aptamer binding functionality.

This successful data demonstrating aptamer siRNA efficacy against CCR5 tropic HIV-1 substantiated a pilot study using CCR5 tropic HIV-1 infected humanized mice. The chemically synthesized aptamer siRNA conjugates were administered at a dose 2 times that of the original published *in vivo* study to maximize amount of therapeutic injected. Mimicking the published *in vivo* study, aptamer was injected at day one, 24 hours later, and one week later to counteract systemically circulating HIV-1 virions if in case they were sequestering circulating aptamer limiting the amount of cell-aptamer interaction. Surprisingly no anti-HIV-1 effects were observed though there was successful inhibition observed *in vitro*. The lack of aptamer siRNA conjugate efficacy *in vivo* demonstrated the necessity to further validate the chemically synthesized constructs. The published *in vivo* study utilized *in vitro* transcribed aptamer and siRNA RNA that yields different modifications that are made to the ribonucleic acid that vary from that of chemically synthesized products. This variation in sequence modification can affect stability *in vivo* and requires further investigation into the pharmacokinetics of the new constructs.

PART II

MODELING ZIKA PATHOGENESIS IN HUMANIZED MICE

CHAPTER 4

HUMANIZED MOUSE MODEL OF ZIKA VIRUS INFECTION AND PATHOGENESIS

Zika virus is an arthropod-borne flavivirus from the Flaviviridae virus family consisting of positive-stranded RNA envelopes viruses. Related to several other global virus epidemics, including Dengue virus and West Nile virus, Zika virus has become the predominant emerging threat to public health in recent years due to multiple outbreaks in the Asian-Pacific countries and the Americas. The increased incidence and limited mechanistic and epidemiological understanding of the Zika virus spread and pathogenesis has presented the need for development of an animal model to recapitulate viral infection and immune response as seen in infected humans. In this regard, humanized mice, that have been previously demonstrated to be susceptible to Dengue virus infection, will be instrumental in elucidating Zika viral infection pathogenesis. Humanized mouse models, including the huHSC and the BLT models, as well as control immunodeficient non-humanized mice, have successfully demonstrated susceptibility to Zika virus infection with long-term viremia. Preliminary data also suggests a limited antibody response against the Zika viral envelope and capsid proteins produced in the BLT model. These results establish the use of humanized mice as a novel model for Zika virus immunopathogenesis studies.

Introduction

Zika infection and resulting consequences pose a significant concern for public health. Originally isolated in 1947 from a rhesus monkey in the Zika forest of Uganda, human infection cases were rare and recapitulation of the viral infection *in vivo* was tedious due to the limited number of available models and route of infection required to mimic infection, such as intracranial or *in utero* inoculations [112]. As Zika is an arthropod-born virus, the spread of the Aedes mosquito has led to the spread of Zika virus worldwide [113]. Though historic infections have been documented in regions of Africa and Asia, the vector spread has led to an increase in transmission of the virus with most recent outbreaks demonstrated in the Polynesian islands and the Americas [5, 114]. With infection incidence growing, understanding of

transmission routes have increased with transmission through sexual and vertical routes now becoming well-documented in humans and *in vivo* (Fig 18) [115-119]. Resultant infection in adults can present as

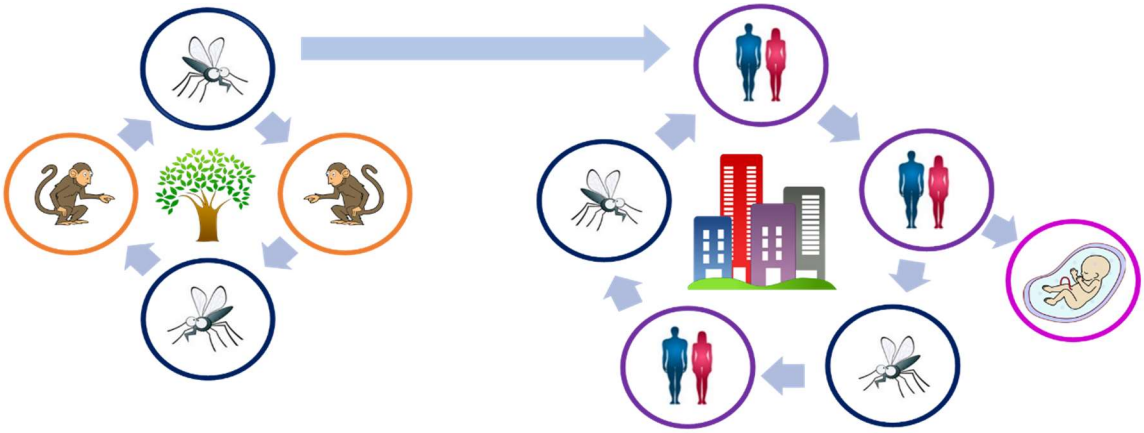

Figure 18 Transmission Cycle of Zika Virus. Enzootic transmission occurred between mosquitoes and non-human primates. The spread of Aedes aegypti and albopictus increased transmission prevalence amongst humans. In recent years, horizontal and vertical transmission between humans have been documented.

Guillain-Barré syndrome, with more severe consequences in fetuses and newborns with infection presenting most notably as microcephaly amongst other congenital birth defects [120-122]. Dramatic infection distribution and severity, especially amongst neonates, have spurred the investigation into animal models that can mimic viral pathogenesis, provide novel insight into mechanisms of dissemination and immune response, and be used to evaluate innovative therapeutic and vaccine approaches [59].

Animal models originally used for Zika infection were limited to wild-type lab mouse strains that required intracranial inoculation to mimic neurological disease in adult and neonatal mice. In more recent years, use of wild type mice inoculated via intravenous, subcutaneous, or intrahepatic routes showed little to no viral replication. These *in vivo* studies revealed that the Zika virus is antagonized by human type I interferon response. Such results led to the use of mice with type I interferon knocked out, known as A129 and AG129 mice [123, 124]. These models can become infected due to innate immune deficiencies and reliably permit Zika virus replication. Infection of A129/AG129 mice as adults results in detectable acute viral replication in multiple tissues, including testes, kidney, brain, eye and bladder. Viral RNA in plasma and urine has also been detected.

Recent studies have also investigated the use of the rhesus macaque monkey as a model for Zika virus infection [125, 126]. Adult rhesus macaques exposed by subcutaneous inoculation develop transient plasma viremia detectable up to 7 days post infection. Viral RNA was detected in various lymphoid tissues, brain, and the reproductive tract up to 35 days post infection. Subsequent analysis of cell subpopulations demonstrated the presence of viral RNA in spleenocyte derived macrophages, dendritic cells, and B cells as well as in axillary lymph node derived macrophages, dendritic cells, B cells, with the rare exception of one monkey demonstrating viral RNA in the T cell population. This study provides evidence that healthy adult rhesus macaques can sustain Zika viral infection with dissemination to the nervous and reproductive tissues. These findings are guiding investigations into the characterization of Zika pathogenesis within these reservoirs. The success of this *in vivo* study and necessity for further investigation is hampered by the limited sample size and excessive cost incurred with use of nonhuman primate model.

While multiple *in vivo* models are currently under investigation to establish the mechanism of infection, replication, and clearance, establishment of a physiologically relevant model has not yet been achieved. Modeling of Zika infection in a system able to recapitulate a true human infection is critical to our understanding of the virus pathology. In this regard, humanized mice provide an ideal setting for investigating Zika virus pathogenesis. The immunodeficient genetic background used for the preparation of the humanized mice, BALB/c-Rag1^{null}γc^{null} or BALB/c-Rag2^{null}γc^{null}, lacks the maturation and expansion capabilities of all mouse lymphocytes; thus, is ideal for transplantation of human cells. Two primary humanized mouse models are widely used for the study of human disease. The first model, the huHSC, is generated by transplantation of human hematopoietic stem cells into immunocompromised neonatal mice. The second model, the BLT, is similarly generated by transplantation of human hematopoietic stem cells into adult immunodeficient mouse but with the addition of human fetal liver and thymus graft placed underneath the kidney capsule. Both models sustain multilineage hematopoiesis with continued de novo development of human immune cells. The BLT model is most noted for high human T cell engraftment, as

these cells undergo T cell education in the autologous thymus graft. This generation of a complete human immune system in the humanized mouse is ideal for evaluation of Zika virus pathogenesis and immune response. To validate the use of humanized mice for the study of Zika viral infection, we employed the huHSC and BLT humanized mouse models in comparison to non-humanized mice of the same genetic background for evaluation of susceptibility to infection, disease pathology, and immune response.

Methods

Generation of huHSC and BLT humanized mice: huHSC mice were generated as previously described [78]. Briefly, BALB/c-Rag1^{null}γc^{null} or BALB/c-Rag2^{null}γc^{null} 1-4 day old neonates were irradiated at a non-lethal dose of 3.5 gy up to 24 hours prior to engraftment. Pups were injected intrahepatically with 0.3-1.0x10^6 CD34 human hematopoietic stem cells. 12 weeks after injection, mice were screened for engraftment by the presence of human lymphocytes.

BLT mice were also generated as previously described [24]. Briefly, BALB/c-Rag1^{null}γc^{null} or BALB/c-Rag2^{null}γc^{null} 5-8 week old mice were irradiated at a non-lethal dose of 3.5 gy up the day of surgery. The day of surgery, human fetal liver and thymus were grafted underneath the kidney capsule of the mice. The following day, the mice are injected intravenously with 0.3-1x10^6 autologous CD34 hematopoietic stem cells. 12 weeks post surgery, mice were screened for engraftment levels of human lymphocytes.

Humanized mouse engraftment analysis: 40µl of blood was collected with heparin via tail vein bleed. 5µl mouse blocking buffer [Normal mouse serum (Jackson Immuno Research Labs), Rat anti-mouse CD16/CD32 (Mouse FC Receptor Monoclonal), Human gamma globulin (Jackson Immuno Research Labs)] was added to each sample, vortexed, and incubated at room temperature for 5-8 minutes. 2µl each of CD45, CD3, and/or CD4, CD14, CD19 was added to each sample, vortexed, and incubated for 30 minutes at room temperature in the dark. Samples were lysed and washed following the Erythrocyte lysing kit and cells were fixed in 1% paraformaldehyde/DPBS for flow analysis. Samples were run on the BD Acurri C6 flow cytometer and analyzed with FlowJo version X. CD45, CD3, and either CD4, CD14 or CD19 cells as

determined by flow cytometry using BD Accuri C6. As it was not known at the time of the first experiment the target cell type or receptor, looking at the pan leukocyte marker (CD45), all T cells (CD3), T helper cells (CD4), monocytes (CD14), and B cells (CD19) was of interest.

Zika virus propagation and mouse infection: Zika Virus Puerto Rico ABC59 strain with a titer of 3.5x107 PFU/mL was a kind gift from Rashika Perera. Virus was further propagated by infection of Vero cells at 80% confluency at an MOI of 0.01. During infection, cells were cultured in DMEM/2% Heat inactivated FBS/ 1x ABAM/ 2Mm L-glutamine. Virus was collected by collection of culture supernatant when CPE, as demonstrated by cell death, affected approximately 50% of the cell population. Virus stock was titered by qRT-PCR.

Adult mice were inoculated with low passage Zika virus by injection of 100 µL via subcutaneous injection in tandem with 100 µL via intraperitoneal injection.

Zika viral load analysis by qRT-PCR: 40 µl of blood was collected via tail vein bleed into EDTA coated tube. 110µl DPBS was added to each tube and mixed. Blood was centrifuged at 300g for 5 minutes. 150µl plasma was transferred to new labeled 1.5ml tube and stored at -80C until RNA extraction. Plasma was thawed and brought to room temperature prior to RNA extraction. RNA was extracted following the Omega E.Z.N.A Viral RNA Extraction kit protocol. RNA was eluted with 20µl DEPC water and stored at -80C.

Viral loads were determined by qRT-PCR using iTaq Universal Probes One-Step kit with the following primers and probe that were optimized from a publication by Lanciotti 2008: Zika1087 5'CCGCTGCCCAACACAAG3', Zika 1108FAM 5'AGCCTACCTTGACAAGCAGTCAGACACTCAA3', Zika 1163c 5'CCACTAACGTTCTTTTGCAGACAT3'[127]. Samples were run using a Bio-Rad C1000 Thermal Cycler with a CFX96 Real-Time System using the following thermocycler protocol: 10 minute 50˚C Reverse Transcriptase step, 3 minute 95˚C Taq activation and DNA denaturation step, 40 cycles of 15 second 95˚C denaturation

and 60 second 58˚C anneal/extend/plate read. Viral loads were determined by comparison with a Zika standard curve.

Immunohistochemistry analysis of mouse tissues: Mouse tissue samples collected for histological analysis included mesenteric lymph node, kidney, human thymus graft if applicable, lung, heart, seminal vesicles, prostate, urethra, penis, bladder, testes, epididymis, whole brain, eye, spleen, and bone marrow. Mouse tissue samples that were initially used for pathology were stored in RNA later. All other pathology samples were collected and fixed in 10% formalin for at least 24 hours, after which the samples were transferred to 70% ethanol for storage. Tissue samples where then embedded into paraffin blocks then sectioned and mounted onto microscope slides for further analysis. Samples were processed following previously established protocol using rabbit polyclonal anti-Zika envelope protein though the kind gift from the CDC.

Antibody detection in humanized mouse plasma immunoprecipitation using S35 labeling: To increase sensitivity, Vero cells were left uninfected or infected with Zika PRV ABC59 at an MOI of 1 or Dengue-2 Jamaica strain. 1-2 days after infection, cells were starved with cysteine/methionine free media and then incubated with S35 labeled cysteine/methionine. Cells were washed and lysate was collected using RIPA. Clarified lysate was mixed with human serum containing antibodies against dengue or humanized mouse plasma, and the subjected to immunoprecipitation by Protein A/G agarose beads. Samples were washed, denatured, and then loaded onto a PAGE gel. Gels were either transferred to PVDF or dried for imaging by a phosphoimager or traditional film.

Humanized mouse antibody determination by native-PAGE and Western blot analysis: Vero cells were either left uninfected or infected with Zika PRV ABC59. Cells were washed, lysed and protein concentration was determined. Zika PRV ABC59 passage 3 viral lysate was also used as a positive control. For the native PAGE, uninfected cell lysate, infected cell lysate, and viral lysate were each loaded at 1 µg, 12.5µg and 25µg to determine limit of detection. Samples were ran on a non-denaturing PAGE gel and

transferred to PVDF membrane. Primary 4G2 pan flavivirus antibody was used as a positive control and mouse plasma from non-humanized, huHSC, and BLT from mice infected for >90 days was used for testing [128]. Appropriate HRP conjugated secondary antibody was used for protein target detection by chemiluminescence.

Western blot analysis was completed on mouse plasma, uninfected cell lysate and infected cell lysate, and viral lysate. Samples were denatured and then ran on an SDS-PAGE gel and transferred to a PVDF membrane. 4G2 and mouse plasma with appropriate secondary antibody were used and the blot was analyzed by chemiluminescence.

Coomassie stain of denatured uninfected cell lysate, infected cell lysate, viral lysate, and humanized mouse plasma ran on a denaturing SDS-PAGE gel. Lanes were analyzed for number and molecular weight of bands present to confirm if antibody and Zika virus proteins were present.

Evaluation of flow cytometry for detection of antibodies in humanized mouse plasma: Plasma samples from infected mice >90 days of infection were tested for use as primary antibodies for detection by flow cytometry. Briefly, Vero cells were infected with Zika PRV ABC59 passage 3 at an MOI of 1 for 24 hours. The cells were collected, fixed and permeabilized using BD Fix/Perm, and blocked with either FBS or goat serum. Cells were either left untreated, incubated with secondary antibody only, or incubated with 4G2 pan flavivirus antibody as a positive control, or mouse plasma at different dilutions. The cells were washed and then incubated with the appropriate fluorophore conjugated secondary antibody for detection by flow cytometry. Cells were washed again and then ran on the BD Acciru C6. Data was analyzed by FloJo version X.

CLARITY imaging: Enhanced fluorescence imaging of whole brains was done initially by forming a tissue-hydrogel hybrid as previously reported (Nature 497:332–337.10.1038/nature12107). Hydrogel-embedded brains were cryosectioned into 180-µm sections containing 2 ml of clearing solution (4% sodium dodecyl sulfate and 200 mM boric acid in deionized water, pH 8.5). Sections were clarified at room

temperature for 4 days, with one change of clearing solution. Sections were then washed twice with 2 ml of TBS for 24 h per wash at room temperature. Washed sections were incubated in TBS containing 1:400 dilution of hyper-immune, anti-Zika polyclonal rabbit serum for two days. Sections were then washed twice with 2 ml of TBS for 24 h per wash at room temperature. Washed sections were incubated in TBS containing 1:2000 dilution of anti-rabbit Alexa555 secondary antibody for two days. Sections were then washed twice with 2 ml of TBS for 24 h per wash at room temperature. Washed sections were incubated in TBS containing 0.01 mg/ml of Hoechst 33342 dye (Molecular Probes, Rockford, IL), washed with TBS, and mounted on positively charged glass slides (VECTASHIELD antifade mounting medium; Vector Laboratories, Burlingame, CA). Images were acquired using a FluoView 1200 scanning-laser confocal microscope (Olympus, Center Valley, PA). Fluorescence was detected for Alexa555 (Zika virus) and Hoechst dye (nuclear counterstain).

Results

Humanized mice and non-humanized mice are susceptible to Zika virus infection and sustain viral loads for greater than 4 months: Surprisingly, non-humanized, huHSC, and BLT mice became infected and sustained viral loads for greater than 4 months. Three separate experiments were conducted to observe viral infection kinetics to demonstrate reproducibility in the models. All 3 experiments demonstrated that mice could become infected by intraperitoneal and subcutaneous inoculation. Non-humanized mice demonstrated infection as early as 2 days post inoculation consistently maintained viral loads around 10^5 Zika RNA copies/mL in mouse plasma for greater than 100 days. The huHSC and BLT humanized mouse models also demonstrated infection as early as 2 days post inoculation and displayed increasing viral loads for approximately 14 days, with a steady downward trend to below the limit of detection (10^3 Zika virus RNA copies/mL) for the qRT-PCR assay between days 60 and 80 post inoculation

(Figure 19 A-B). A few of the remaining huHSC and BLT mice still had detectable viral loads by week 30 post inoculation. Representative infection data from BLT, huHSC, and non-humanized mice is presented. Examination of viral transmission via mucosal challenges of the 3 mouse models suggest that mucosal challenge is inefficient as infection was irregularly positive at various time points and was intermittently detected for at least 70 days. In the third experiment, 2 out of the 5 non-humanized mice challenged rectally, and 2 of the 5 challenged vaginally became positive for infection with sporadic positive timepoints. huHSC mice displayed a similar viral load trend to that of experiment 1 and 2. One out of 2

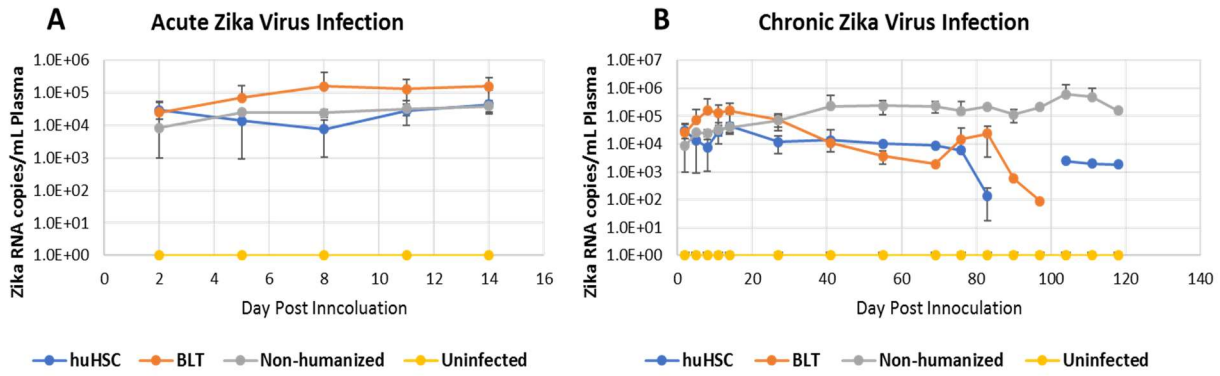

Figure 19 Zika Virus Infection Kinetics A) All mice were inoculated with Zika Virus Puerto Rican ABC59 strain by intraperitoneal and subcutaneous routes. A) Representative data of acute Zika virus infection B) Representative data of chronic Zika virus infection.

mice for both rectal and vaginal challenged became positive. For the BLT model, 1 out of 2 mice for rectal challenge appear positive, while none of the vaginally challenged mice have any detectable viremia at any time point.

The pan 4G2 flavivirus antibody recognized the Zika viral envelope using native-PAGE: The native PAGE gel using the 4G2 antibody recognized the Zika envelope. Target was identified in both Zika infected Vero cell lysate and Zika viral lysate in a protein dependent amount down to 12.5µg. The uninfected Vero cell lysate did not have any banding. The antibody used on mouse plasma from non-humanized, huHSC, and BLT used at a dilution of 1:50 was unable to detect any Zika protein. This suggests that if antibody is present, the limit of detection is too high by native-PAGE.

A denaturing PAGE gel was run with Zika viral lysate, uninfected and Zika virus infected Vero cell lysate and mouse plasma samples, and then stained with coomassie blue to observe protein banding. The objective was to observe heavy and light chain antibody produced in the humanized mice, as well as matching Zika virus protein banding between Zika viral lysate, Zika virus infected vero cell lysate, and infected mouse plasma lysate. After coomassie staining, neither Zika virus proteins nor antibody were seen in mouse plasma by SDS-PAGE. To determine if analysis by Western blot would increase the limit of detection, a Western blot was run in the same manner as the native-PAGE. The results yielded no banding from any of the mouse plasma samples. Data not shown.

Humanized mouse plasma cannot be used for detection of primary antibody by flow cytometry: The pan 4G2 antibody was validated for detection of Zika virus infection in Vero, BHK, and THP-1 immortalized cell lines by flow cytometry. To determine if humanized mouse plasma could be used as a primary antibody for detection of Zika virus infection in immortalized cells, Zika infected Vero cells were incubated with mouse plasma. A fluorophore-conjugated secondary antibody targeting human IgG and IgM was used for flow cytometry analysis. Unfortunately, the secondary antibody had high nonspecific binding at various dilution ratios requiring further optimization.

Preliminary data suggests the potential for antibody production in Zika infected BLT mice: Multiple immunoprecipitation experiments have been conducted utilizing humanized and non-humanized mouse plasma collections ranging from 3 to 16 weeks post inoculation. Preliminary results suggest that BLT mice are producing antibody targeting the Zika envelope and capsid proteins. Further experiments are needed to confirm findings.

Immunohistochemistry revealed novel pathological findings in Zika infected mice: An interesting discovery in BLT mice infected with Zika virus was seen in the human thymus graft from terminal tissues of mice that were infected for extended periods (Fig 20 A-D). The BLT mice, that are surgically implanted with human liver and thymus under their kidney capsule, revealed a hemorragic thymus graft upon dissection (Fig 20 B-D). Further evidence is needed to determine if there is a correlation between Zika infection and thymus graft hemorrhage. IHC data on Zika infected BLT mouse tissues samples have been promising. Zika virus antigen was detected in the human thymus graft in what appears to be mononuclear cells with morphology indicative of human myeloid cells (Figure 20 B). Lymphocyte infiltration and severe human thymic damage was observed in Zika infected mice as compared to the negative control. Cells positive for Zika virus antigen include endothelial cells and perivascular macrophages and fibroblasts surround the renal tubules (Fig 21 B-C) as well as interstitial positive macrophages and fibroblasts within the human thymus graft (Fig 21 D). Further investigation revealed circulating monocytes with strong immunoreactivity within the blood vessel of the human

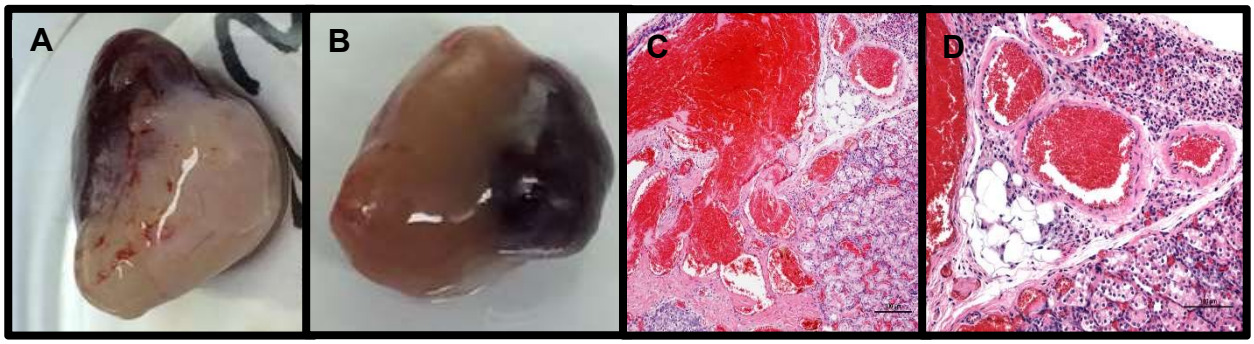

Figure 20 Zika virus related pathogenesis. A) Healthy human thymus graft from an uninfected BLT mouse. B) Hemmoragic thymus graft from Zika virus infected BLT mouse. C) Ruptured blood vessels and inflammation and cell infiltration present within human thymus graft of a Zika virus infected BLT mouse. D) Thrombus in a small sized blood vessel with substantial amounts of cell infiltration and inflammation.

thymus graft suggesting that the infection is cell associated (Fig 21 E). Cell-associated viremia present on a circulating monocyte can give rise the infection of blood vessel endothelial cells that can then transmit the infection to perivascular fibroblasts and macrophages (Fig 21 F-G). Zika virus antigen was also observed in the brain of these long-term infected mice. Immunoreactivity was observed in perivascular

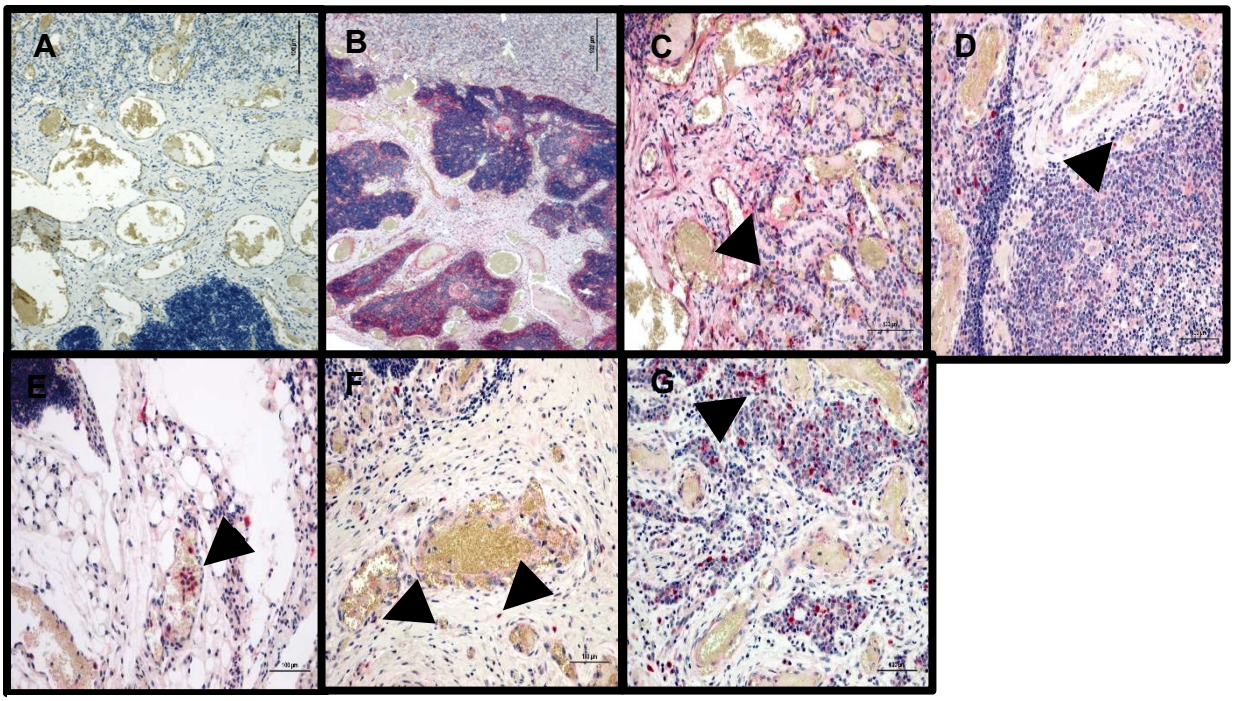

Figure 21 Immunohistochemistry for Zika virus envelope protein of human thymus graft from BLT mouse. A) Uninfected thymus graft. B) Strong immunoreactivity for Zika virus envelope protein as seen by red coloring. C) Immunoreactivity seen in macrophages, fibroblasts and endothelial cells in mouse kidney. D) Immunoreactivity seen in macrophages and fibroblasts in human thymus graft. E) Immunoreactivity seen in circulating monocytes within a blood vessel of the human thymus graft suggesting cell associated viremia. F-G) Additional immunoreactivity seen in fibroblasts, endothelial cells and macrophages in the human thymus graft.

microglial cells surrounding blood vessels within the brain (Fig 22 A). This infection can be seen spread to the hippocampus in glial cells, astrocytes, and neuron, with hippocampal degeneration in the A1 layer (Figure Fig 22B)). Viral antigen was also detected in the cerebral cortex and substantia nigra, with astrocytes, microglia cells, and neurons appearing to be targets (Figure Fig 22 C-D).

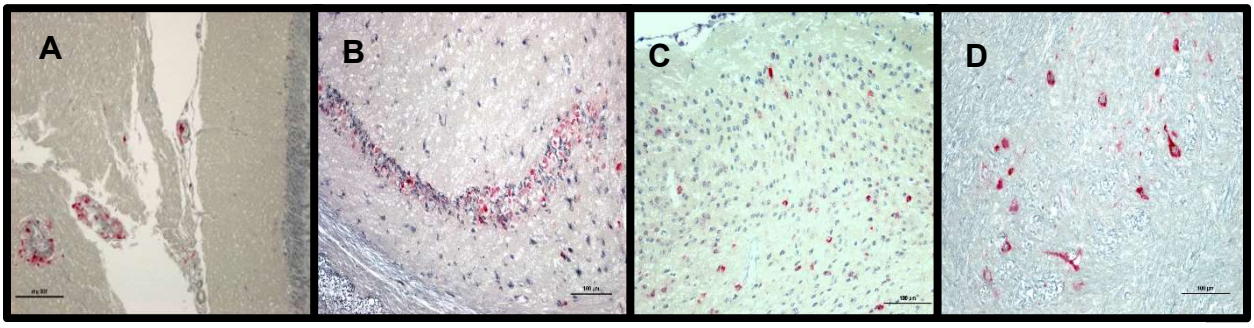

Figure 22 Immunohistochemistry for Zika virus in Brain from chronically infected BLT mice. A) Immunoreactivity see in microglial cells surround blood vessels in the brain. B) Zika antigen detected in glial cells and neurons in the hippocampus with degeneration seen in the A1 layer. C) Immunoreactivity in glial cells, astrocytes, and neurons in the cerebral cortex. D) Zika viral antigen seen in neurons of the substantia nigra.

Analysis of non-humanized, huHSC, and BLT mice that had terminal tissues collected during the acute phase of infection, day 7 and 14 post inoculation, revealed additional pathological data. The most pronounced gross observation of non-humanized mouse tissues during terminal tissue collection was adematous lungs. The huHSC mice overall had normal tissue appearance with the exception of one mouse collected 14 days post inoculation that appeared to have mottled dark red lungs. In contrast to the long-term infected BLT mice, only one BLT mouse collected 7 days post inoculation demonstrated a small hemorrhage within the human thymus graft at the renal vein. Further analysis by IHC as well as CLARITY studies will be completed on all tissue types collected and analyzed for dissemination of Zika virus.

Discussion

With the reemergence and increased spread of Zika infection worldwide, a great need for an *in vivo* model capable of recapitulating infection mechanics and immune response has become necessary. Multiple *in vivo* models have been studied for use in Zika infection but require genetic modifications, as seen in the A129/AG129 mouse models, or excessive costs and limited sample size as observed in the use of nonhuman primate models. To address the need of a physiologically relevant model encompassing a complete human immune system that enables high samples sizes at a much more reasonable cost, we have employed the use of the humanized mouse model for modeling of Zika of pathogenesis.

In contrast to the previous mouse models used to demonstrate Zika virus infection, the humanized mice and non-humanized mice used in this study sustained viremia for greater than 4 months. The non-humanized mice infected by intraperitoneal and subcutaneous routes continually sustained the highest levels of viral loads over the course of the experimental period. This is likely due to the fact that they contain only an innate immune system with no adaptive immunity to recognize and clear the infection. The huHSC and BLT mice that were inoculated by intraperitoneal and subcutaneous routes demonstrated peak viremia by 14 days post infection with continual decline for the remainder of the experiment. Transmission of the virus via subcutaneous/intraperitoneal routes was highly efficient, whereas infection

by vaginal and rectal challenges resulted in a small percentage of mice becoming infected, with detectable viral loads occurring in an intermittent manner. Successful demonstration of viral infection by vaginally challenges is promising for future studies examining maternal-fetal and sexual transmission.

Viral infection with a consistent trend in viral load decline after 21 days post infection in the huHSC and BLT humanized mouse models is suggestive of a mounting adaptive immune response. Immunoprecipitations of humanized mouse plasma for human antibodies have provided preliminary data suggesting that BLT mice are generating a successful antibody response against the Zika viral infection. Further examination into the Zika specific antibody response seen in BLT mice will require an increase in the sample size as well as examination of a wide array of time points to determine when detectable human antibody levels are present in the mouse plasma [129].

Histological analysis of Zika infected mouse tissues from both humanized and non-humanized mice have provided evidence regarding cellular and tissue targets and dissemination as related to infection pathology observed in human patients. Initial findings have demonstrated the presence of Zika viral proteins in the brain and human thymus graft of BLT mice that had been infected for 4 to 10 weeks. Gross pathology of the human thymus graft showed substantial hemorrhage in the Zika infected mice, whereas there were not any noticeable pathologies in the uninfected BLT mice. Examination by H&E staining of the thymic tissue revealed substantial lymphocyte infiltration and vascular degeneration. After examination by IHC, positive staining of mononuclear cells with morphology indicative of monocytes, macrophages, fibroblasts, and endothelial cells was observed. Figure 21 E showed positive immunoreactivity of monocytes within the blood vessels of the thymus graft suggesting that Zika virus is cell associated and that subsequent viral dissemination throughout the body is completed by cell-associated viral transmission from circulating monocytes to blood vessel endothelial cells, that is then carried to fibroblasts and macrophages within the tissues. Investigation into the potential for Zika viral protein presence in the brain was then conducted. The results revealed viral antigen in the areas of the

hippocampus, cerebral cortex, and substantia nigra with prominent cell targets appearing to be microglial cells, astrocytes, and neurons. Degenerative changes were readily observed in the A1 layer of the hippocampus. Degeneration in this area can lead to markedly diminished neuronal capacity. This type of neuropathogenesis is a historical attribute of Zika viral infection in both fetal and adult infections. The most notable type of abnormality associated with Zika virus infection is microcephaly observed in human fetus and newborns exposed to the pathogen. Successful detection of Zika viral proteins in the brains of the BLT mice suggest that this is an ideal model for investigation into maternal-fetal transmission studies and subsequent fetal brain development defects.

Multiple other tissues examined from the BLT humanized mice have demonstrated positive signal for Zika viral proteins. As it was recently shown that the infection can spread via sexual transmission, investigation into the male reproductive tract was critical. IHC results revealed viral antigen in the testes collected from Zika infected BLT mice. Viral antigen was found within the interstitial cells with no significant antigen present within the seminiferous tubules. This data suggests that Zika infection is not transmitted via infected sperm, rather it is more likely that Zika virus is spread through the seminal fluids. Other specific tissue reservoirs harboring Zika virus include the kidney and bladder of the mice. This corroborates other studies wherein Zika viral RNA has been detected in urine for extended periods of time. The current hypothesis is that because Zika virus can be found in urine, the addition of the human thymus graft acts as a reservoir to exacerbate infection by causing leukocyte infiltrates to rupture capillaries found in the graft. Additional other tissues where viral antigen was discovered include the eye, lung, and heart. Further investigation is required to determine the significance of these tissue reservoirs for Zika viral replication, though increasing evidence as seen in the tissue sections is suggesting that the virus is cell-associated as opposed to circulating cell-free virions.

As intensive effort into the understanding of Zika virus infection, persistence, and transmission continues, the characterization of animal models to better reflect viral pathogenesis remains an important

priority. Although multiple animal models have been demonstrated to be successful in sustaining viral infection and modeling pathogenesis, they come with many limitations. Current published mouse models require genetic manipulation of the mouse innate immune system in order to become susceptible to Zika virus infection. Nonhuman primate models on the other hand, are completely immunocompetent and are ideal for investigation into potential vaccine approaches for protection against infection. However, these models are quite costly and limited the sample size available for experimentation. To address the need of an immunocompetent animal model that comes with a much more feasible cost, we have investigated the use of humanized mice for modeling Zika infection. Able to demonstrate viral infection with the potential for an immune response as well as histopathology observed tissues critical for viral persistence, our preliminary studies suggest that humanized mice will prove to be an essential animal model for the study of Zika viral pathogenesis.

While both humanized and non-humanized became infected with Zika virus and maintain persistent infection for more than 4 months, the humanized mice showed a steady downward trend in viral loads begin around 40 days post inoculation indicative of a mounting immune response. Humanized mice, and in particular the BLT model as the human T cells are educated in a human thymus permitting recognition of MHC II by human antigen presenting cells, contain a complete functioning innate and adaptive immune system allowing examination of a host immune response to Zika virus infection. Additionally, the presence of human immune cells results in drug metabolism representative of that of a human patient. Altogether, humanized mice present a sound platform for the investigation of Zika virus pathogenesis and potential therapeutics for treatment of the infection.

CONCLUSION

Humanized mice are important preclinical models for investigation of human pathogens, evaluation of infection mechanisms and immune responses. Additionally, they act as a platform to better understand therapeutics and vaccination studies. The study of HIV-1 has highly benefited from the development of humanized mice. The ability to establish and disseminate infection throughout the humanized mouse has provided a solid foundation for research into viral latency and therapeutic treatment methods.

Humanized Mice for the Study of HIV-1

Establishment of humanized mice for HIV-1 viral latency studies has led to the development of the humanized mouse viral outgrowth assay for detection of latent HIV-1. Acting as an ultrasensitive model for detection of latent HIV-1 from donor cells, humanized mice have enabled the establishment of a more sensitive means for detection of viral outgrowth from CD4 T cell samples from HIV-1 positive donors. By direct comparison of the humanized mouse viral outgrowth assay (hmVOA) to that of the gold standard quantitative viral outgrowth assay (qVOA), the sensitivity level of the hmVOA was ascertained. First using donor CD4 T cells that were positive for viral outgrowth by the qVOA, the hmVOA was determined to be as sensitive in detecting viral outgrowth as all donor samples used resulted in viral outgrowth *in vivo*. Next, to determine if the hmVOA was more sensitive, the study proceeded with donor CD4 T cell samples that were negative by the qVOA. Out of the five donors that had no detectable viral outgrowth by the qVOA, 4 of the donors had viral outgrowth in the hmVOA model. Detection of HIV-1 from samples that had undetectable virus using an ultrasensitive *in vivo* model is an incredible success for the field. As the field shifts towards development of a cure for HIV-1, an assay that can detect ultra-low levels of replication competent virus is critical. With the ability to detect latent HIV-1, the hmVOA enables the verification of curative strategies success. Prominent curative attempts, such as the “Boston Patients” and the “Mississippi Baby” who have had cell samples stored from multiple time points, can have samples

tested by the hmVOA to further establish the sensitivity and importance of the hmVOA for latent HIV-1 detection.

Increased sensitivity in latent HIV-1 detection will enable the evaluation of various other cell types that are theorized to harbor latent replication competent HIV-1, as well as multiple tissue reservoirs from HIV-1 positive donors to be investigated as potential latent reservoirs. However, the success of the hmVOA brings to light certain limitations that are innate to the state of HIV-1 latency. While CD4 T cells are the most researched reservoir harboring latent HIV-1, it is not guaranteed that the rare latent cells will be captured in the peripheral blood cells that are used for viral outgrowth analysis. This limitation requires investigation into other potential tissue reservoirs that are limited by donor participation and the ability to biopsy specific tissue types considered to be potential latent reservoirs.

The pathogenesis and detection of HIV-1 in humanized mice provides a significant advantage into the efficacy determination of novel therapeutics for the treatment of HIV-1. Due to the physiological relevance and recapitulation of a complete immune system, humanized mice have enabled the ability to characterize the efficacy of gene therapy for the modulation of HIV-1 infection. Conditionally replicating vectors harboring anti-HIV payloads have been studied as a therapy to control HIV-1 on a cellular basis without the need for continued therapeutic treatments. Conditionally replicating vectors are developed through the modification of a lentivirus that only encodes an anti-HIV payload. This anti-HIV payload, containing either shRNA or CRISPR/Cas9, is able to intracellularly modulate HIV-1 infection, as well as repackage into mature virions. This replaces the virulent HIV-1 genome permitting spread of the HIV-1 inhibitory payload, such as CRISPR/Cas9 or siRNA, to other cells. *In vitro*, conditionally replicating vectors harboring shRNA against the HIV-1 LTR and Tat/Rev were successful in inhibiting HIV-1 replication in primary human CD4 T cells. Surprisingly, the CRISPR/Cas9 construct targeting a NFkB doublet in the LTR region was not efficacious, which is hypothesized to be due to the low transduction efficiency and the ability of HIV-1 to overcome non-homologous end joining disruptions in the genetic sequence. Translation

in vivo harnessed the unique ability of the huPBL model to generate humanized mice from conditionally replicating vector transduced cells. huPBL mice generated from transduced cells containing anti-HIV constructs failed to modulate HIV-1 infection. The lack of success with these vectors *in vivo* demonstrates the need to further refine the vectors to increase transduction levels and generate robust repackaging capabilities. In total, success of future generations of conditionally replicating vectors will rely on vectors ability to stably maintain selective pressures on HIV-1 viral replication.

In contrast to using gene therapy as a tool to modulate HIV-1 infection, development of a systemically administered therapeutic regimen that has reduced toxicity and immunogenicity has prompted investigation into aptamer constructs. Aptamers, single-stranded nucleic acids that form specific high affinity tertiary structures, can act as both an antibody like molecule capable of virus neutralization as well as a delivery system for small non-coding RNA. Previously published work demonstrated that an aptamer construct directed towards the gp120 envelope protein of HIV-1 was capable of virus neutralization and was efficacious in delivering siRNA targeting HIV-1 Tat/Rev. These results were demonstrated in the huHSC humanized mouse model marked by a decrease in HIV-1 RNA copies present in the plasma and a recovery of CD4 T cells levels. To build upon this study, a new siRNA construct targeting the NFkB doublet in the HIV-1 LTR was developed. Surprisingly, when the previously validated Tat/Rev siRNA and new LTR siRNA aptamer conjugates were administered *in vivo* to CXCR4 infected huHSC mice no anti-HIV effects were observed. Subsequent *in vitro* experiments demonstrated that the aptamer construct was efficacious only against CCR5 tropic HIV-1. Following this notion, a pilot study using CCR5 tropic HIV-1 infected huHSC mice was conducted. No HIV-1 inhibition was observed *in vivo*. These results bring to light the necessity for further evaluation of the sequence and modifications required for pharmacokinetic stability and efficacy of the aptamer constructs. Use of the huHSC humanized mouse model has yielded crucial data regarding the functionality and stability of these approaches, allowing future studies to build upon the findings discovered in these experiments to

generate a new generation of gene therapy and aptamer approaches that are better suited for inhibition of HIV-1 infection.

Humanized Mice for the Study of Zika Virus

In addition to investigation of HIV-1, the Flaviviridae family of viruses has also benefited from the use of humanized mice. Many foundational studies investigating Dengue virus provided novel insight into the mechanistic mode of infection and subsequent immune response. Recently, this model has been employed for research into the reemerging Zika virus. New understandings regarding cell and tissue targets, immune response, and infection kinetics were brought about by implementing humanized mice for demonstration of Zika infection. The Puerto Rican Zika virus strain successfully infected adult huHSC and BLT humanized mice as well as non-humanized mice from the same genetic background. The virus demonstrated strong kinetics during the acute phase of infection, with detectable plasma RNA levels ranging from 10^3 to 10^6 RNA copies/mL. Whereas previous studies using interferon knockout mice and non-human primates had limited detectable viral loads only for a brief period, the huHSC, BLT, and non-humanized mice maintained detectable viral loads for greater than 4 months. Sporadic viral loads, that are seen during the chronic phase of infection are a common trend among all *in vivo* models suggesting that plasma viral loads are not a stable reservoir for viral replication, which is consistent with the hypothesis derived from the immunohistochemistry data from infected BLT mice that Zika virus is cell associated and that viral loads would be better ascertained from analysis of whole blood.

Zika viral dissemination was observed throughout various tissues by immunohistochemistry through detection of Zika envelope protein. Unique tissue reservoirs for Zika virus replication being noted in the BLT model. Detection of the Zika virus envelope protein within the humanized mouse tissues appears to be predominantly cell-associated suggesting that spread of infection is due to cell-associated virus being transmitted from circulating monocytes to blood vessel endothelial cells and subsequent tissue fibroblasts and macrophages. IHC of the brain from chronically infected BLT mice revealed cellular targets

consisting of microglial cells, astrocytes, and neurons in the hippocampus, cerebral cortex and substantia nigra. Future studies will be able to harness the unique abilities of humanized mice to sustain viral infection for extended periods of time to investigate sexual and maternal-fetal transmission. Additionally, potential therapeutics for the treatment or prevention of infection can be examined using humanized mice [130]. The success and novel insight provided by humanized mice have paved the way for the use of humanized mice as an instrumental model for the study of viral pathogenesis.

Beyond the field of infectious disease research, humanized mice have also been critical for the recapitulation of human cancer and the evaluation of cell therapies for treatment of multiple human diseases. Use of immunodeficient IL-2 knockout mice have permitted the engraftment of the number of primary human cancers, such as the growth of melanoma lung metastases, breast cancer, and adult T-cell leukemia and lymphoma. These humanized mouse studies demonstrated central characteristics of human disease including maintenance and expansion of the cancer as well as novel insight into human immune responses against the disease.

As humanized mice are transplanted with hematopoietic stem cells or mature immune cells, investigation into the treatment of multiple human diseases by modification of the transplanted cells has become possible. This *in vivo* model has proved important for determination of the safety and efficacy of cell therapies, including that of lentiviral vector modified T cells. Innovative approaches for modifying the immune system to target specific disease has resulted in the generation of chimeric antigen receptor engineer T cell therapy. This novel therapy constructs a T cell receptor with specificity for specific antigen, resulting in a T cell able to be directed to any target of interest. This method of gene therapy is commonly evaluated in the huPBL model. Current progress using humanized mice has shown that T cell therapy may prove to be a viable option for treatment of leukemia. Such understanding has paved the way for cell therapy approaches for treatment of other diseases.

With all the success that has been made using the various humanized mouse models for disease research, there are still several limitations that exist. As the current immunodeficient mouse models are engineered to have knockouts for all adaptive immune cells, the enduring innate immune system within the mouse continues to hinder human engraftment levels. Various new models of humanized mice are currently being developed to diminish mouse innate immune cells as well as enhance development of human innate immune cells. This enhancement is generated by the knockin of various human cytokine genes, such as M-CSF and GM-CSF, to increase the development of the myeloid lineage [131]. A second limitation results from the lack of human specific secondary lymphoid structures that decrease in the ability for a robust humoral immune response. As T cell reconstitution is limited, with class switching unavailable in the huHSC model and only limited class switching in the BLT model, antibody-mediated responses are unlikely to be consistently observed. Modifications to the genetic background of the humanized mice will need to be investigated to promote the humanized mouse as a solid model for development and testing vaccine studies.

Additional modifications to the genetic immunodeficient mouse background will continue to improve the ability of humanized mice to fully recapitulate human specific infection and disease. The establishment of a more complete human immune system will make further insights into human diseases possible. Altogether, humanized mice have a promising future as a vital tool for use in translational research in the fields of infectious disease, cancer, and cell therapy research.

REFERENCES

1. McGonigle, P. and B. Ruggeri, *Animal models of human disease: challenges in enabling translation.* Biochemical pharmacology, 2014. **87**(1): p. 162-71.
2. Shultz, L.D., F. Ishikawa, and D.L. Greiner, *Humanized mice in translational biomedical research.* Nature reviews. Immunology, 2007. **7**(2): p. 118-30.
3. Akkina, R., *New generation humanized mice for virus research: comparative aspects and future prospects.* Virology, 2013. **435**(1): p. 14-28.
4. Policicchio, B.B., I. Pandrea, and C. Apetrei, *Animal Models for HIV Cure Research.* Front Immunol, 2016. **7**: p. 12.
5. Fauci, A.S. and D.M. Morens, *Zika Virus in the Americas--Yet Another Arbovirus Threat.* The New England journal of medicine, 2016. **374**(7): p. 601-4.
6. Brehm, M.A., et al., *Generation of improved humanized mouse models for human infectious diseases.* Journal of immunological methods, 2014. **410**: p. 3-17.
7. Akkina, R., et al., *Humanized Rag1-/- gammac-/- mice support multilineage hematopoiesis and are susceptible to HIV-1 infection via systemic and vaginal routes.* PloS one, 2011. **6**(6): p. e20169.
8. Kuruvilla, J.G., et al., *Dengue virus infection and immune response in humanized RAG2(-/-)gamma(c)(-/-) (RAG-hu) mice.* Virology, 2007. **369**(1): p. 143-52.
9. Garcia, J.V., *Humanized mice for HIV and AIDS research.* Current opinion in virology, 2016. **19**: p. 56-64.
10. Bosma, G.C., R.P. Custer, and M.J. Bosma, *A severe combined immunodeficiency mutation in the mouse.* Nature, 1983. **301**(5900): p. 527-30.
11. Mosier, D.E., et al., *Transfer of a functional human immune system to mice with severe combined immunodeficiency.* Nature, 1988. **335**(6187): p. 256-9.

12. McCune, J.M., et al., *The SCID-hu mouse: murine model for the analysis of human hematolymphoid differentiation and function.* Science, 1988. **241**(4873): p. 1632-9.

13. Lapidot, T., et al., *Cytokine stimulation of multilineage hematopoiesis from immature human cells engrafted in SCID mice.* Science, 1992. **255**(5048): p. 1137-41.

14. Shultz, L.D., et al., *Multiple defects in innate and adaptive immunologic function in NOD/LtSz-scid mice.* Journal of immunology, 1995. **154**(1): p. 180-91.

15. Christianson, S.W., et al., *Role of natural killer cells on engraftment of human lymphoid cells and on metastasis of human T-lymphoblastoid leukemia cells in C57BL/6J-scid mice and in C57BL/6J-scid bg mice.* Cell Immunol, 1996. **171**(2): p. 186-99.

16. Ito, M., et al., *NOD/SCID/gamma(c)(null) mouse: an excellent recipient mouse model for engraftment of human cells.* Blood, 2002. **100**(9): p. 3175-82.

17. Mombaerts, P., et al., *RAG-1-deficient mice have no mature B and T lymphocytes.* Cell, 1992. **68**(5): p. 869-877.

18. Shinkai, Y., et al., *RAG-2-deficient mice lack mature lymphocytes owing to inability to initiate V (D) J rearrangement.* Cell, 1992. **68**(5): p. 855-867.

19. Gimeno, R., et al., *Monitoring the effect of gene silencing by RNA interference in human CD34+ cells injected into newborn RAG2-/- gammac-/- mice: functional inactivation of p53 in developing T cells.* Blood, 2004. **104**(13): p. 3886-93.

20. Kenney, L.L., et al., *Humanized mice and tissue transplantation.* American journal of transplantation: official journal of the American Society of Transplantation and the American Society of Transplant Surgeons, 2016. **16**(2): p. 389.

21. Yuan, J., et al., *Zinc-finger nuclease editing of human cxcr4 promotes HIV-1 CD4+ T cell resistance and enrichment.* Molecular Therapy, 2012. **20**(4): p. 849-859.

22. Perez, E.E., et al., *Establishment of HIV-1 resistance in CD4+ T cells by genome editing using zinc-finger nucleases.* Nature biotechnology, 2008. **26**(7): p. 808-816.

23. McCune, J.M. and L.D. Shultz, *Humanized mice as models for human disease*, in *Humanized Mice for HIV Research*. 2014, Springer. p. 15-24.

24. Veselinovic, M., P. Charlins, and R. Akkina, *Modeling HIV-1 Mucosal Transmission and Prevention in Humanized Mice.* Methods in molecular biology, 2016. **1354**: p. 203-20.

25. Traggiai, E., et al., *Development of a human adaptive immune system in cord blood cell-transplanted mice.* Science, 2004. **304**(5667): p. 104-7.

26. Berges, B.K., et al., *Mucosal transmission of R5 and X4 tropic HIV-1 via vaginal and rectal routes in humanized Rag2-/- gammac -/- (RAG-hu) mice.* Virology, 2008. **373**(2): p. 342-51.

27. Veselinovic, M., et al., *Mucosal tissue pharmacokinetics of the integrase inhibitor raltegravir in a humanized mouse model: Implications for HIV pre-exposure prophylaxis.* Virology, 2016. **489**: p. 173-8.

28. Veselinovic, M., et al., *HIV pre-exposure prophylaxis: mucosal tissue drug distribution of RT inhibitor Tenofovir and entry inhibitor Maraviroc in a humanized mouse model.* Virology, 2014. **464-465**: p. 253-63.

29. Denton, P.W. and J.V. Garcia, *Humanized mouse models of HIV infection.* AIDS Rev, 2011. **13**(3): p. 135-48.

30. Berges, B.K., et al., *Humanized Rag2(-/-)gammac(-/-) (RAG-hu) mice can sustain long-term chronic HIV-1 infection lasting more than a year.* Virology, 2010. **397**(1): p. 100-3.

31. Wege, A.K., et al., *Functional and phenotypic characterization of the humanized BLT mouse model.* Current topics in microbiology and immunology, 2008. **324**: p. 149-65.

32. Karpel, M.E., C.L. Boutwell, and T.M. Allen, *BLT humanized mice as a small animal model of HIV infection.* Current opinion in virology, 2015. **13**: p. 75-80.

33. Vatakis, D.N., et al., *Using the BLT humanized mouse as a stem cell based gene therapy tumor model.* J Vis Exp, 2012(70): p. e4181.

34. Marsden, M.D., et al., *HIV latency in the humanized BLT mouse.* Journal of virology, 2012. **86**(1): p. 339-47.

35. McCarthy, M., *WHO sets out $56m Zika virus response plan.* BMJ, 2016. **352**: p. i1042.

36. Walsh, N.C., et al., *Humanized Mouse Models of Clinical Disease.* Annu Rev Pathol, 2017. **12**: p. 187-215.

37. Fujiwara, S., K. Imadome, and M. Takei, *Modeling EBV infection and pathogenesis in new-generation humanized mice.* Exp Mol Med, 2015. **47**: p. e135.

38. Ginwala, R., et al., *HTLV-1 Infection and Neuropathogenesis in the Context of Rag1-/-gammac-/-(RAG1-Hu) and BLT Mice.* J Neuroimmune Pharmacol, 2017.

39. Denton, P.W., O.S. Sogaard, and M. Tolstrup, *Using animal models to overcome temporal, spatial and combinatorial challenges in HIV persistence research.* J Transl Med, 2016. **14**: p. 44.

40. Brainard, D.M., et al., *Induction of robust cellular and humoral virus-specific adaptive immune responses in human immunodeficiency virus-infected humanized BLT mice.* Journal of virology, 2009. **83**(14): p. 7305-21.

41. Melkus, M.W., et al., *Humanized mice mount specific adaptive and innate immune responses to EBV and TSST-1.* Nature medicine, 2006. **12**(11): p. 1316-22.

42. Watanabe, S., et al., *Hematopoietic stem cell-engrafted NOD/SCID/IL2Rgamma null mice develop human lymphoid systems and induce long-lasting HIV-1 infection with specific humoral immune responses.* Blood, 2007. **109**(1): p. 212-8.

43. Veselinovic, M., et al., *Topical gel formulation of broadly neutralizing anti-HIV-1 monoclonal antibody VRC01 confers protection against HIV-1 vaginal challenge in a humanized mouse model.* Virology, 2012. **432**(2): p. 505-10.

44. Zhou, J., et al., *Cell-specific RNA aptamer against human CCR5 specifically targets HIV-1 susceptible cells and inhibits HIV-1 infectivity.* Chem Biol, 2015. **22**(3): p. 379-90.

45. Takahashi, M., J.C. Burnett, and J.J. Rossi, *Aptamer-siRNA chimeras for HIV.* Adv Exp Med Biol, 2015. **848**: p. 211-34.

46. Neff, C.P. and R. Akkina, *Targeted Delivery of Aptamers and siRNAs for HIV Prevention and Therapies in Humanized Mice*, in *Humanized Mice for HIV Research*. 2014, Springer. p. 397-406.

47. Zhou, J., et al., *Functional in vivo delivery of multiplexed anti-HIV-1 siRNAs via a chemically synthesized aptamer with a sticky bridge.* Mol Ther, 2013. **21**(1): p. 192-200.

48. Neff, C.P., et al., *An aptamer-siRNA chimera suppresses HIV-1 viral loads and protects from helper CD4(+) T cell decline in humanized mice.* Sci Transl Med, 2011. **3**(66): p. 66ra6.

49. Zhou, J., et al., *Selection, characterization and application of new RNA HIV gp 120 aptamers for facile delivery of Dicer substrate siRNAs into HIV infected cells.* Nucleic acids research, 2009. **37**(9): p. 3094-109.

50. Tebas, P., et al., *Gene editing of CCR5 in autologous CD4 T cells of persons infected with HIV.* The New England journal of medicine, 2014. **370**(10): p. 901-10.

51. Maier, D.A., et al., *Efficient clinical scale gene modification via zinc finger nuclease-targeted disruption of the HIV co-receptor CCR5.* Hum Gene Ther, 2013. **24**(3): p. 245-58.

52. Banerjea, A., et al., *Inhibition of HIV-1 by lentiviral vector-transduced siRNAs in T lymphocytes differentiated in SCID-hu mice and CD34+ progenitor cell-derived macrophages.* Mol Ther, 2003. **8**(1): p. 62-71.

53. Shimizu, S., S.S. Yadav, and D.S. An, *Stable Delivery of CCR5-Directed shRNA into Human Primary Peripheral Blood Mononuclear Cells and Hematopoietic Stem/Progenitor Cells via a Lentiviral Vector.* Methods in molecular biology, 2016. **1364**: p. 235-48.

54. Li, M.-J., et al., *Long-term inhibition of HIV-1 infection in primary hematopoietic cells by lentiviral vector delivery of a triple combination of anti-HIV shRNA, anti-CCR5 ribozyme, and a nucleolar-localizing TAR decoy.* Molecular Therapy, 2005. **12**(5): p. 900-909.

55. Levine, B.L., et al., *Gene transfer in humans using a conditionally replicating lentiviral vector.* Proceedings of the National Academy of Sciences of the United States of America, 2006. **103**(46): p. 17372-7.

56. Evans, J.T. and J.V. Garcia, *Lentivirus vector mobilization and spread by human immunodeficiency virus.* Hum Gene Ther, 2000. **11**(17): p. 2331-9.

57. Mathew, A. and R. Akkina, *Dengue Viral Pathogenesis and Immune Responses in Humanized Mice*, in *Humanized Mice for HIV Research*. 2014, Springer. p. 469-479.

58. Frias-Staheli, N., et al., *Utility of humanized BLT mice for analysis of dengue virus infection and antiviral drug testing.* Journal of virology, 2014. **88**(4): p. 2205-2218.

59. Morrison, T.E. and M.S. Diamond, *Animal Models of Zika Virus Infection, Pathogenesis, and Immunity.* Journal of virology, 2017. **91**(8).

60. Archin, N.M., et al., *Eradicating HIV-1 infection: seeking to clear a persistent pathogen.* Nature reviews. Microbiology, 2014. **12**(11): p. 750-64.

61. Deeks, S.G., et al., *International AIDS Society global scientific strategy: towards an HIV cure 2016.* Nature medicine, 2016. **22**(8): p. 839-50.

62. Alexaki, A., Y. Liu, and B. Wigdahl, *Cellular reservoirs of HIV-1 and their role in viral persistence.* Current HIV research, 2008. **6**(5): p. 388-400.

63. Brenchley, J.M., et al., *T-cell subsets that harbor human immunodeficiency virus (HIV) in vivo: implications for HIV pathogenesis.* Journal of virology, 2004. **78**(3): p. 1160-8.

64. Tyagi, M., R.J. Pearson, and J. Karn, *Establishment of HIV latency in primary CD4+ cells is due to epigenetic transcriptional silencing and P-TEFb restriction.* Journal of virology, 2010. **84**(13): p. 6425-37.

65. Eisele, E. and R.F. Siliciano, *Redefining the viral reservoirs that prevent HIV-1 eradication.* Immunity, 2012. **37**(3): p. 377-88.

66. Brenchley, J.M., et al., *CD4+ T cell depletion during all stages of HIV disease occurs predominantly in the gastrointestinal tract.* The Journal of experimental medicine, 2004. **200**(6): p. 749-59.

67. Howell, A.L., et al., *Human immunodeficiency virus type 1 infection of cells and tissues from the upper and lower human female reproductive tract.* Journal of virology, 1997. **71**(5): p. 3498-506.

68. Cillo, A.R. and J.W. Mellors, *Which therapeutic strategy will achieve a cure for HIV-1?* Current opinion in virology, 2016. **18**: p. 14-9.

69. Spina, C.A., et al., *An in-depth comparison of latent HIV-1 reactivation in multiple cell model systems and resting CD4+ T cells from aviremic patients.* PLoS pathogens, 2013. **9**(12): p. e1003834.

70. Rosenbloom, D.I., et al., *Designing and Interpreting Limiting Dilution Assays: General Principles and Applications to the Latent Reservoir for Human Immunodeficiency Virus-1.* Open Forum Infect Dis, 2015. **2**(4): p. ofv123.

71. Procopio, F.A., et al., *A Novel Assay to Measure the Magnitude of the Inducible Viral Reservoir in HIV-infected Individuals.* EBioMedicine, 2015. **2**(8): p. 874-83.

72. Henrich, T.J., et al., *Antiretroviral-free HIV-1 remission and viral rebound after allogeneic stem cell transplantation: report of 2 cases.* Ann Intern Med, 2014. **161**(5): p. 319-27.

73. Persaud, D., et al., *Absence of detectable HIV-1 viremia after treatment cessation in an infant.* The New England journal of medicine, 2013. **369**(19): p. 1828-35.

74. Luzuriaga, K., et al., *Viremic relapse after HIV-1 remission in a perinatally infected child.* New England Journal of Medicine, 2015. **372**(8): p. 786-788.

75. Siliciano, J.D. and R.F. Siliciano, *Enhanced culture assay for detection and quantitation of latently infected, resting CD4+ T-cells carrying replication-competent virus in HIV-1-infected individuals.* Methods in molecular biology, 2005. **304**: p. 3-15.

76. Chun, T.W., et al., *Gene expression and viral prodution in latently infected, resting CD4+ T cells in viremic versus aviremic HIV-infected individuals.* Proceedings of the National Academy of Sciences of the United States of America, 2003. **100**(4): p. 1908-13.

77. Malnati, M.S., et al., *A universal real-time PCR assay for the quantification of group-M HIV-1 proviral load.* Nat Protoc, 2008. **3**(7): p. 1240-8.

78. Berges, B.K., et al., *HIV-1 infection and CD4 T cell depletion in the humanized Rag2-/-gamma c-/- (RAG-hu) mouse model.* Retrovirology, 2006. **3**: p. 76.

79. Rouet, F., et al., *Transfer and evaluation of an automated, low-cost real-time reverse transcription-PCR test for diagnosis and monitoring of human immunodeficiency virus type 1 infection in a West African resource-limited setting.* Journal of clinical microbiology, 2005. **43**(6): p. 2709-17.

80. Shan, L. and R.F. Siliciano, *From reactivation of latent HIV-1 to elimination of the latent reservoir: the presence of multiple barriers to viral eradication.* BioEssays : news and reviews in molecular, cellular and developmental biology, 2013. **35**(6): p. 544-52.

81. Hill, A.L., et al., *Real-Time Predictions of Reservoir Size and Rebound Time during Antiretroviral Therapy Interruption Trials for HIV.* PLoS pathogens, 2016. **12**(4): p. e1005535.

82. Metcalf Pate, K.A., et al., *A Murine Viral Outgrowth Assay to Detect Residual HIV Type 1 in Patients With Undetectable Viral Loads.* The Journal of infectious diseases, 2015. **212**(9): p. 1387-96.

83. Yuan Z, K.G., Lu W, Li Q, *Reactivation of HIV-1 provirses in immune-compromised mice engrafted with human VOA-negative CD4+ T cells.* Journal of Virus Eradication, 2017. **3**: p. 61-65.

84. Bukovsky, A.A., J.P. Song, and L. Naldini, *Interaction of human immunodeficiency virus-derived vectors with wild-type virus in transduced cells.* Journal of virology, 1999. **73**(8): p. 7087-92.

85. Dropulic, B., M. Hermankova, and P.M. Pitha, *A conditionally replicating HIV-1 vector interferes with wild-type HIV-1 replication and spread.* Proceedings of the National Academy of Sciences of the United States of America, 1996. **93**(20): p. 11103-8.

86. Tebas, P., et al., *Antiviral effects of autologous CD4 T cells genetically modified with a conditionally replicating lentiviral vector expressing long antisense to HIV.* Blood, 2013. **121**(9): p. 1524-33.

87. Morris, K.V. and J.J. Rossi, *Anti-HIV-1 gene expressing lentiviral vectors as an adjunctive therapy for HIV-1 infection.* Current HIV research, 2004. **2**(2): p. 185-191.

88. Weinberg, M.S., et al., *The antisense strand of small interfering RNAs directs histone methylation and transcriptional gene silencing in human cells.* RNA, 2006. **12**(2): p. 256-62.

89. Suzuki, K., et al., *Promoter Targeting shRNA Suppresses HIV-1 Infection In vivo Through Transcriptional Gene Silencing.* Mol Ther Nucleic Acids, 2013. **2**: p. e137.

90. Turner, A.W., J. De La Cruz, and K.V. Morris, *Mobilization-competent Lentiviral Vector-mediated Sustained Transcriptional Modulation of HIV-1 Expression.* Mol Ther, 2009. **17**(2): p. 360-368.

91. Turner, A.M., et al., *Characterization of an HIV-targeted transcriptional gene-silencing RNA in primary cells.* Hum Gene Ther, 2012. **23**(5): p. 473-83.

92. Novina, C.D., et al., *siRNA-directed inhibition of HIV-1 infection.* Nature medicine, 2002. **8**(7): p. 681-6.

93. Saayman, S.M., et al., *Potent and targeted activation of latent HIV-1 using the CRISPR/dCas9 activator complex.* Molecular Therapy, 2015.

94. Limsirichai, P., T. Gaj, and D.V. Schaffer, *CRISPR-mediated activation of latent HIV-1 expression.* Molecular Therapy, 2016. **24**(3): p. 499-507.

95. Ye, L., et al., *Seamless modification of wild-type induced pluripotent stem cells to the natural CCR5Δ32 mutation confers resistance to HIV infection.* Proceedings of the National Academy of Sciences, 2014. **111**(26): p. 9591-9596.

96. Hou, P., et al., *Genome editing of CXCR4 by CRISPR/cas9 confers cells resistant to HIV-1 infection.* Scientific reports, 2015. **5**: p. 15577.

97. Choi, J., et al., *Lentivirus pre-packed with Cas9 protein for safer gene editing.* Gene therapy, 2016. **23**(7): p. 627-633.

98. Zhu, W., et al., *The CRISPR/Cas9 system inactivates latent HIV-1 proviral DNA.* Retrovirology, 2015. **12**(1): p. 22.

99. Kaminski, R., et al., *Negative feedback regulation of HIV-1 by gene editing strategy.* Scientific reports, 2016. **6**.

100. Tiscornia, G., O. Singer, and I.M. Verma, *Production and purification of lentiviral vectors.* NATURE PROTOCOLS-ELECTRONIC EDITION-, 2006. **1**(1): p. 241.

101. Ueda, S., et al., *Anti-HIV-1 potency of the CRISPR/Cas9 system insufficient to fully inhibit viral replication.* Microbiology and immunology, 2016. **60**(7): p. 483-496.

102. Wang, G., et al., *CRISPR-Cas9 can inhibit HIV-1 replication but NHEJ repair facilitates virus escape.* Molecular Therapy, 2016.

103. Wang, Z., et al., *CRISPR/Cas9-derived mutations both inhibit HIV-1 replication and accelerate viral escape.* Cell reports, 2016. **15**(3): p. 481-489.

104. Bobbin, M.L., J.C. Burnett, and J.J. Rossi, *RNA interference approaches for treatment of HIV-1 infection.* Genome Med, 2015. **7**(1): p. 50.

105. Berkhout, B., *RNA interference as an antiviral approach: targeting HIV-1.* Curr Opin Mol Ther, 2004. **6**(2): p. 141-5.

106. de Fougerolles, A., et al., *Interfering with disease: a progress report on siRNA-based therapeutics.* Nat Rev Drug Discov, 2007. **6**(6): p. 443-53.

107. Swamy, M.N., H. Wu, and P. Shankar, *Recent advances in RNAi-based strategies for therapy and prevention of HIV-1/AIDS.* Advanced drug delivery reviews, 2016. **103**: p. 174-186.

108. Zhou, J. and J. Rossi, *Aptamers as targeted therapeutics: Current potential and challenges.* Nature Reviews Drug Discovery, 2016.

109. Thiel, K.W. and P.H. Giangrande, *Intracellular delivery of RNA-based therapeutics using aptamers.* Therapeutic delivery, 2010. **1**(6): p. 849-861.

110. Whatley, A.S., et al., *Potent inhibition of HIV-1 reverse transcriptase and replication by nonpseudoknot,"UCAA-motif" RNA aptamers.* Molecular Therapy-Nucleic Acids, 2013. **2**: p. e71.

111. Moore, M.D., et al., *Protection of HIV neutralizing aptamers against rectal and vaginal nucleases: implications for RNA-based therapeutics.* The Journal of biological chemistry, 2011. **286**(4): p. 2526-35.

112. Dick, G., S. Kitchen, and A. Haddow, *Zika virus (I). Isolations and serological specificity.* Transactions of the Royal Society of Tropical Medicine and Hygiene, 1952. **46**(5): p. 509-520.

113. Chouin-Carneiro, T., et al., *Differential Susceptibilities of Aedes aegypti and Aedes albopictus from the Americas to Zika Virus.* PLoS Negl Trop Dis, 2016. **10**(3): p. e0004543.

114. Ioos, S., et al., *Current Zika virus epidemiology and recent epidemics.* Medecine et maladies infectieuses, 2014. **44**(7): p. 302-307.

115. Musso, D., et al., *Potential sexual transmission of Zika virus.* Emerg Infect Dis, 2015. **21**(2): p. 359-61.

116. Besnard, M., et al., *Evidence of perinatal transmission of Zika virus, French Polynesia, December 2013 and February 2014.* Euro surveill, 2014. **19**(13): p. 20751.

117. Musso, D., et al., *Potential for Zika virus transmission through blood transfusion demonstrated during an outbreak in French Polynesia, November 2013 to February 2014.* Euro surveill, 2014. **19**(14): p. 20761.

118. Yockey, L.J., et al., *Vaginal Exposure to Zika Virus during Pregnancy Leads to Fetal Brain Infection.* Cell, 2016. **166**(5): p. 1247-1256 e4.

119. Foy, B.D., et al., *Probable non-vector-borne transmission of Zika virus, Colorado, USA.* Emerg Infect Dis, 2011. **17**(5): p. 880-2.

120. Cao-Lormeau, V.-M., et al., *Guillain-Barré Syndrome outbreak associated with Zika virus infection in French Polynesia: a case-control study.* The Lancet, 2016. **387**(10027): p. 1531-1539.

121. Mlakar, J., et al., *Zika virus associated with microcephaly.* The New England journal of medicine, 2016. **2016**(374): p. 951-958.

122. Hickman, H.D. and T.C. Pierson, *Zika in the Brain: New Models Shed Light on Viral Infection.* Trends in molecular medicine, 2016. **22**(8): p. 639-41.

123. Rossi, S.L., et al., *Characterization of a novel murine model to study Zika virus.* The American journal of tropical medicine and hygiene, 2016. **94**(6): p. 1362-1369.

124. Dowall, S.D., et al., *A Susceptible Mouse Model for Zika Virus Infection.* PLoS Negl Trop Dis, 2016. **10**(5): p. e0004658.

125. Dudley, D.M., et al., *A rhesus macaque model of Asian-lineage Zika virus infection.* Nature communications, 2016. **7**.

126. Hirsch, A.J., et al., *Zika Virus infection of rhesus macaques leads to viral persistence in multiple tissues.* PLoS pathogens, 2017. **13**(3): p. e1006219.

127. Lanciotti, R.S., et al., *Genetic and serologic properties of Zika virus associated with an epidemic, Yap State, Micronesia, 2007.* Emerg Infect Dis, 2008. **14**(8): p. 1232-9.

128. Priyamvada, L., et al., *Human antibody responses after dengue virus infection are highly cross-reactive to Zika virus.* Proceedings of the National Academy of Sciences of the United States of America, 2016. **113**(28): p. 7852-7.

129. Villaudy, J., et al., *Critical assessment of human antibody generation in humanized mouse models.* Journal of immunological methods, 2014. **410**: p. 18-27.

130. Retallack, H., et al., *Zika virus cell tropism in the developing human brain and inhibition by azithromycin.* Proceedings of the National Academy of Sciences of the United States of America, 2016. **113**(50): p. 14408-14413.

131. Honeycutt, J.B., et al., *HIV persistence in tissue macrophages of humanized myeloid-only mice during antiretroviral therapy.* Nature medicine, 2017. **23**(5): p. 638-643.